EXPERIMENTAL DETERMINATION OF THE FLOW PARAMETERS INVOLVED IN MOISTURE MIGRATION THROUGH FIBERGLASS INSULATION MATERIALS

by

Dean M. Weekes

Thesis submitted to the Faculty of the
Virginia Polytechnic Institute and State University
in partial fulfillment of the requirements for the degree of

MASTER OF SCIENCE

in

Mechanical Engineering

APPROVED:

W. C. Thomas, Chairman

R. J. Onega

T. E. Diller

March, 1983

Blacksburg, Virginia

EXPERIMENTAL DETERMINATION OF THE FLOW PARAMETERS INVOLVED IN MOISTURE MIGRATION THROUGH FIBERGLASS INSULATION MATERIALS

by

Dean M. Weekes

(ABSTRACT)

An experimental investigation was made to determine the role of gravitational and surface tension forces in the migration of liquid water through fiberglass insulation materials. Straightforward experimental procedures were devised to effectively isolate and quantify flow parameters considered important in describing the flow mechanisms involved. The study was conducted to supplement an earlier investigation into the thermal performance of wetted insulation materials.

Darcy's Law was found to apply for the regime of flow encountered in which liquid water flows under the force of its own weight in horizontal rooftop insulation. Experimental determination of the constant of proportionality in Darcy's Law, the hydraulic conductivity, is all that is needed to describe the migration of liquid water in saturated fiberglass insulation.

Capillary forces, originally thought to play a significant role in the movement of liquid water through fiberglass insulation, were found to be negligible. Capillary rise up a column of insulation measured no higher than 13 mm.

ACKNOWLEDGMENTS

The author would like to express his gratitude to Dr. W. C. Thomas for his guidance and support given during the preparation of this thesis. Thanks are extended to Dr. R. J. Onega and Dr. T. E. Diller for serving on the advisory committee. Acknowledgments are also in order for: E. C. Overstreet, for his photographic assistance in preparing some of the figures; Dr. Michael L. Ulica, for his guidance in the use of the Amray^{R} 900 scanning electron microscope; Joe Wack, Dot Cogan, Bink McInteer, Kelly Leppink, and Guy D'esterre, the boys in the chemical engineering lab who provided an unending supply of distilled water; and his mother, without whose encouragement and moral support this work would not have been possible.

TABLE OF CONTENTS

TABLE OF CONTENTS
(Continued)

LIST OF FIGURES

LIST OF TABLES

NOMENCLATURE

A	=	flow area, m^2
d	=	fiber diameter, m
D_p	=	particle diameter, m
g	=	acceleration of gravity, m/s^2
K	=	hydraulic conductivity, m^2
L	=	length in the direction of flow, m
m	=	hydraulic diameter, m
m_i	=	mass of constituent i, kg
$\dot{m}$	=	mass flow rate, kg/s
n_i''	=	mass flux of constituent i, kg/m^2-s
p	=	pressure, kPa
Q	=	volumetric flow rate, m^3/s
S	=	area of particle surface per unit volume of packed space, m^{-1}
S_t	=	area of particle surface per unit volume, including wall surface, m^{-1}
t	=	time, s
T	=	temperature, C
V	=	flow velocity, m/s
$\forall$	=	volume, m^3
$\forall_i'''$	=	volume fraction of constituent i (per unit total fiberglass volume)
x	=	coordinate, m
z	=	coordinate, m

NOMENCLATURE
(Continued)

β_3	=	capillary rise coefficient, kPa
γ_3	=	thermal diffusivity coefficient, kPa/C
ε	=	porosity of dry insulation (fractional void space)
μ_3	=	dynamic viscosity of liquid, kg/m-s
ρ_i	=	density of constituent i, kg/m^3

Subscripts

1	=	water vapor
2	=	air
3	=	liquid water
4	=	fiberglass matrix material

CHAPTER I

INTRODUCTION

The presence of moisture in rooftop insulation has been shown to have a degrading effect upon thermal performance (1).* Recent work has been concerned with quantifying this effect with respect to heat loss or heat gain in moist insulation. In hopes of gaining a better understanding of the problem, the mechanisms which govern the migration of water (both liquid and vapor) in wetted fiberglass insulation have been studied. Analytical methods for describing the flow mechanisms involved in moist insulation have been hampered by a lack of information concerning material properties. In particular, investigators have been able to correlate the heat transfer results in moist insulation except where there is movement of water in liquid form through the insulation.

The literature (2, 3) suggests that the equations of motion and energy in porous media are strongly linked due to the dominance of the evaporation-condensation flow mechanism -- the transport of water in the vapor phase under a thermal gradient. In his research dealing with the analysis of heat and mass transfer mechanisms in wetted fiberglass insulation materials, Bal (1) has shown that moisture migration in insulation is principally a result of the vapor pressure gradient. However, the model proposed by Thomas, et al. (4) for predicting the

---

*Numbers in parentheses indicate references.

thermal performance of wetted insulation materials breaks down at high moisture concentrations (m_3/m_4 greater than 150 percent). Thomas suggests the need for information concerning the role of capillary and gravitational forces in moisture transport.

This investigation is concerned with the development of a model which accurately predicts the bulk movement of liquid water through insulation. The development of a straightforward experimental procedure to effectively measure the flow parameters of interest will be presented. Attention will be given to flow rates over a range normally encountered in horizontal rooftop insulation materials. Experimental determination of the phenomenological parameters involved in the proposed model will be the ultimate goal of this research. A better understanding of the phenomena affecting flow through porous materials will hopefully be gained through this investigation.

1.1 Description of Insulations Tested

The insulations studied in this investigation are (open) glass fiber insulations made of inorganic glass fibers preformed into semi-rigid rectangular board 51 mm thick. Three types of insulation, all manufactured by Owens/Corning Fiberglas^R, were studied. The manufacturer's designation for the three insulations are Series 703, Series 705, and AF Roof, which are hereafter referred to as insulations A, B, and C, respectively.

In order to examine the lay of the insulation fibers and to get an idea of the general quality of the fibers, photomicrographs were taken.

Figure 1 shows photomicrographs of the samples studied, as viewed through an Amray^{R} 900 scanning electron microscope. Fiber diameter measurements were made from viewings at a higher magnification. The values in Table 1 represent an average diameter calculated from a number of different fiber diameter measurements within a sample. Reported density values represent an average of a number of measurements made in the laboratory among different samples. Nominal density values as supplied by the manufacturer are listed for comparison. Differences as high as 26 per cent between maximum and minimum measurements of density were reported for insulation A. Insulation B showed a 13 per cent difference, while insulation C measurements differed by as much as 18 per cent. Porosity values were calculated from the following relation:

$$\varepsilon = 1 - \frac{\rho_{meas}}{\rho_{fibers}} \quad , \qquad (1)$$

where the density of the fibers used to manufacture the insulation is reported to be 2184 kg/m^3 (4).

1.2 Review of Literature

The study of flow through porous media applies to a large number of disciplines. Soils scientists and ground water hydrologists study the movement of water through different geologic formations in an effort to design effective drainage and irrigation systems. Petroleum engineers track the movement of oil displaced by gas and water through rock

Figure 1. Magnified View of Insulation Samples, 100x.

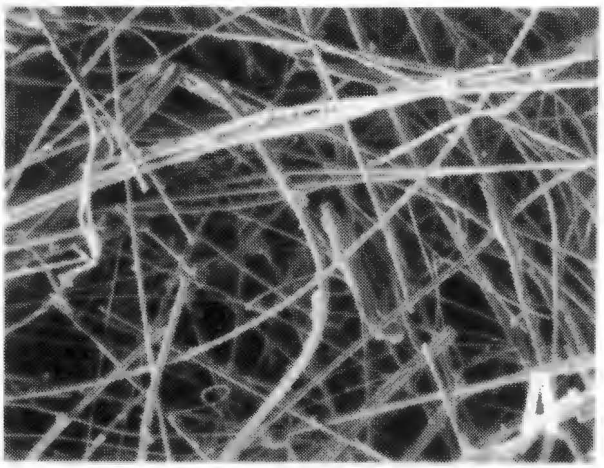
A

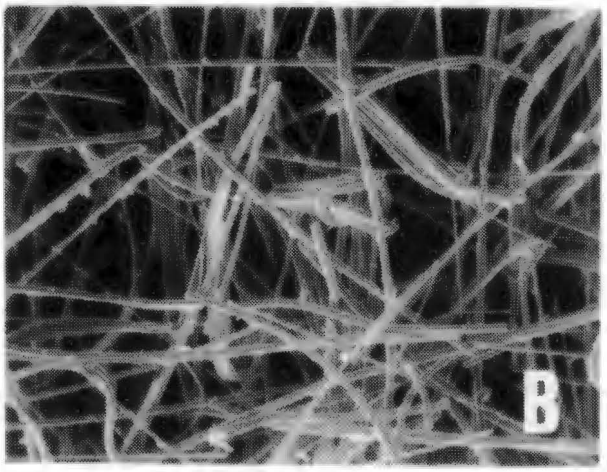
B


C

Table 1. Physical Properties of Insulations Tested.

Manufacturer: Owens/Corning

Insulation	Commercial Designation	Measured Density, ρ (kg/m^3)	Nominal Density, ρ * (kg/m^3)	Porosity, ε (per cent)	Fiber Diameter, d (m)
A	703	50.7	48.1	97.7	12.5×10^{-6}
B	705	108.6	96.1	95.0	19.0×10^{-6}
C	AF Roof	120.3	NA	94.5	20.5×10^{-6}

* From Reference 5.

interstices in order to improve oil recovery methods. Chemical engineers apply their knowledge of flow through porous media in studying adsorption, chromatography, and filtration. All of these disciplines are concerned with the development of mathematical expressions to describe the flow of fluids through porous media.

In what was perhaps the first recorded treatise on flow through porous media, Henry Darcy, in 1856, related the flow of water through a porous medium to the pressure drop across that medium in his study of flow through sand filters in the fountains of the city of Dijon, France (6). This first recorded treatment of the subject was founded strictly on an experimental basis, and Darcy correlated his data to yield the expression

$$Q = \frac{KA}{\mu} \left(- \frac{\Delta p}{L} \right) \qquad (2)$$

where K is a constant of proportionality defined as the hydraulic conductivity, a flow parameter characteristic of the porous medium.

Subsequent investigations concerned with flow through porous media have been varied and cover a range of applications. Much attention has been given to the experimental determination of hydraulic conductivities for a wide range of porous media. In addition, a great deal of research has been conducted to study the range of validity of this law with regards to different flow regimes (laminar, transition, and turbulent) and different classes of porous media. Recent work has been aimed at a theoretical development of the equations governing the flow of fluids through porous media. These equations are generally more complex in

form than Eq. 2 but reduce to Darcy's Law when qualifying assumptions are made.

Upon inspection of Darcy's Law (Eq. 2), one can experimentally determine the K-value of a porous medium by measuring the pressure drop across a porous bed of known cross-sectional area when percolated by a fluid at a given flow rate. A common apparatus designed to carry out this measurement is shown in Fig. 2. While experimental techniques differ slightly among researchers, the concept remains the same. Muskat (7) gives an extensive listing of sandstone hydraulic conductivities which range from 5.0×10^{-16} - 3.0×10^{-12} m^2*. Carman (8) reports hydraulic conductivity values for a number of different porous materials including berl saddles (1.3×10^{-7} - 3.9×10^{-7} m^2), wire crimps (3.8×10^{-9} - 1.0×10^{-8} m^2), silica powder (1.3×10^{-14} - 5.1×10^{-14} m^2), and loose sand beds (2.0×10^{-11} - 1.8×10^{-10} m^2). Hydraulic conductivity values like these exist in the literature for a wide variety of porous materials. Unfortunately, the treatment given the experimental measurement of hydraulic conductivities of fiberglass insulating materials is limited. Wiggins, et al. (9) calculated K-values in the range of 2.4×10^{-11} - 5.1×10^{-11} m^2 in their work to deduce specific surface area of fibrous materials from hydraulic conductivity measurements.

---

*The dimension of hydraulic conductivity is a length squared. SI units are sq m, while some branches of science employ the 'darcy' with

$$1 \text{ darcy} = 9.87 \times 10^{-13} \text{ m}^2.$$

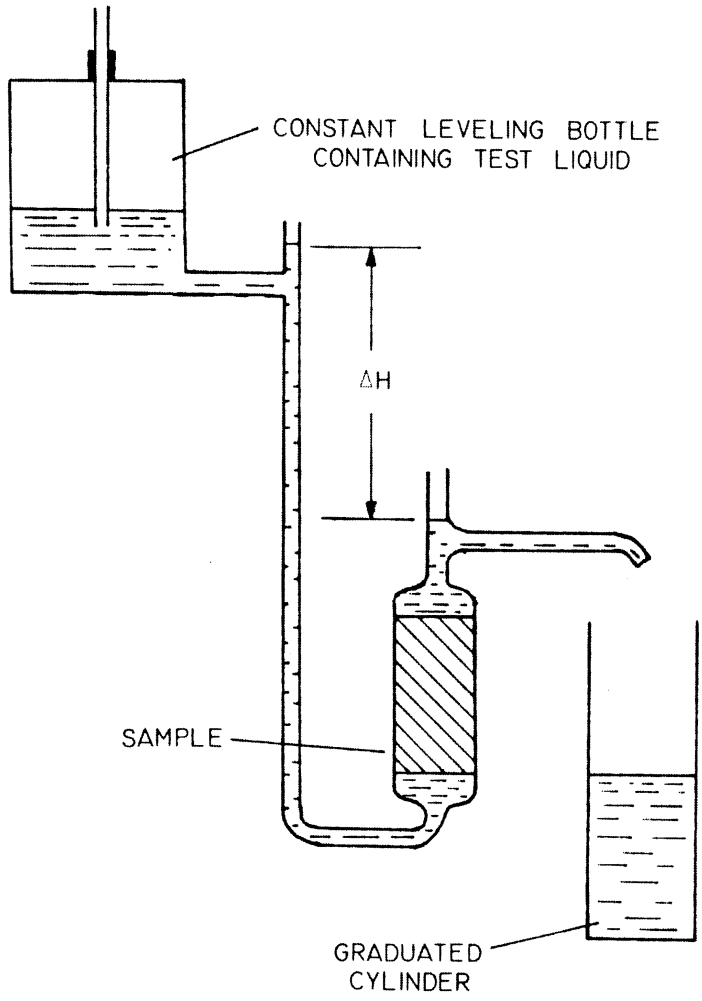

Figure 2. A Hydraulic Conductivity Apparatus.

These hydraulic conductivities all apply to flows in which Darcy's Law successfully correlates the experimental data. However, research has shown that in cases where inertial effects play an important role, as in high flow rates or in high-porosity media, Darcy's Law no longer holds as the hydraulic conductivity ceases to be a constant of proportionality linearly relating flow rate to pressure drop across a porous medium. In the so-called 'non-Darcy' flow regime, different expressions have been proposed to correlate the experimental results. All of these expressions represent the pressure drop for flow through porous media as the sum of two terms, one linear in the velocity (viscous contribution) and the second quadratic in the velocity (inertia contribution).

Forcheimer (10) was the first to replace the linear Darcy Law with the nonlinear expression

$$-\frac{dp}{dx} = a\mu V + b\rho V^2 \tag{3}$$

where a and b are constants for a given medium, determined by experiment. It can be seen from the above expression that Eq. 3 reduces to Darcy's Law for low flow rates, with $a = 1/K$. In studying the pressure drop for high-velocity gaseous flows through porous media of different microstructures, Koh, et al. (11) correlated their data to yield

$$a = \frac{SC_1}{2m\varepsilon(1-\varepsilon)^n}, \quad b = \frac{SC_1C_2}{2\varepsilon^2(1-\varepsilon)^{2n}} \tag{4}$$

where C_1, C_2, and n are constants. Beavers, et al. (12) chose to correlate their data using

$$a = \frac{1}{K}, \qquad b = \frac{c}{\sqrt{K}} \tag{5}$$

where c = 0.074 for porous media made up of metallic fibers which do not have free ends within the medium. Beavers constructed graphs of $(-dp/dx)/\mu V$ versus $\rho V/\mu$ to form linear relationships from which K and b could be determined. More generally, Ergun (13) proposed that

$$a = \frac{150(1-\varepsilon)^2}{\varepsilon^3 D_p^2}, \qquad b = \frac{1.75(1-\varepsilon)}{\varepsilon^3 D_p} \tag{6}$$

for flows through beds of granular solids in both the Darcy and non-Darcy regimes.

Others researching pressure drop data through porous media have chosen to graphically depict their findings on a plot similar to the Moody diagram for pipe flow. Carman (8), Brownell and Katz (14), and Rose (15) plot a modified friction factor versus a modified Reynolds number in their works with flows through packed beds. In these studies, the characteristic dimension in the modified Reynolds number is generally chosen as the average diameter of the non porous solids which make up the porous matrix. A characteristic dimension for a material whose structure is as complex as fiberglass insulation has not been defined.

An alternative theory for hydraulic conductivity determination was proposed by Iberall (16), who treated the walls of the pores of a porous medium as obstacles to an otherwise straight flow of a viscous fluid. Contrary to the constant hydraulic conductivity predicted by Darcy's Law, Iberall's theory suggests that the K-value increases gradually as the fluid velocity increases. The 'drag theory' of hydraulic

conductivity is expected to give good results for highly porous media such as fibers. Iberall relates the pressure drop through a packed bed of fibers to the flow velocity by the expression

$$\frac{\Delta p}{L} = \frac{16\mu V}{3} \frac{(1-\varepsilon)}{\varepsilon d^2} \frac{\left[4 - \ell n \frac{dV\rho}{\mu\varepsilon}\right]}{\left[2 - \ell n \frac{dV\rho}{\mu\varepsilon}\right]} . \qquad (7)$$

As can be seen, the numerous attempts to correlate fluid flow data through porous media are generally of the same form but substantially different in appearance to warrant a theoretical approach to the entire flow problem. While virtually no attention has been given to theoretically studying the complex mechanisms of flow through fiberglass insulation, the subject has been addressed for a few classes of porous media. Huang et al (2) presented a rigorous analysis of the basic equations for mass and heat transfer derived from the laws of physics in their study of drying of hydrated cement paste slabs. Huang noted that when water is in the pendular state, liquid threads in the porous system become progressively discontinuous, and liquid islands form inside the porous system. In coupling the mass and energy transfer processes, he was able to show that when water is in the pendular state, both diffusion and evaporation-condensation mechanisms govern the drying process. An earlier treatment was given by Ceaglske and Hougen (17) with particular reference to drying of granular solids. These authors concluded that the predominant means of moisture transfer in sands is

due to capillary forces and not to moisture concentration gradients as predicted by Fick's diffusion law.

Luikov (3) emphasized the interrelation between liquid and heat transfer in a capillary-porous body in developing the differential equations for transport phenomena in heat pipes. The author pointed to the fact that liquid is transferred not only under the action of a volumetric liquid concentration gradient but also under that of a temperature gradient.

Gray and O'Neill (18) apply the technique of local volume averaging to the equations of motion to describe flow in porous media. For an isotropic medium, the authors claim that only five experimental parameters need be evaluated to model non-Darcian flow of a Newtonian fluid in which the convective and inertial terms are important. Whitaker (19) extended the volume averaging technique in his development of the transport equations for liquid and vapor phases in the drying of porous media. With particular reference to the liquid phase equation of motion, he assumes a flow dependent entirely on gravity and surface tension forces. With these assumptions, Whitaker reports three phenomenological parameters that need be evaluated by experiment to describe the flow process, a more attractive proposal than that given by Gray and O'Neill.

A review of the literature has shown that the experimentally determined coefficient defined in Darcy's Law, the hydraulic conductivity, is of prime importance in characterizing flow through porous media. With particular reference to flow through fiberglass insulation materials, it

will become necessary to measure hydraulic conductivities in the regime of flow of practical importance -- that in which water flows under its own weight in a roof installation. A worst case condition would be that in which the insulation is fully saturated.

It will be the aim of the experiments in this investigation to determine which correlation from the literature for hydraulic conductivity determination (Darcy, non-Darcy, or drag theory) adequately predicts pressure drop data presented herein. The dependence of hydraulic conductivity upon flow rate will be addressed. It should be stressed that non-Darcy behavior is attributed to inertial effects in flows through porous media. These effects are normally felt at higher flow rates. However, inertial effects are also expected to be a factor in lower flow rates through highly porous media such as fibrous materials.

The literature has also shown that capillary forces, while playing a significant role in the drying of granular solids, may not be important when water is in the pendular state throughout a porous matrix. It is recognized that in a nonsaturated porous medium, capillary pressure is the mechanism which maintains water in an immobile, pendular state. When local liquid movement occurs through nonsaturated fiberglass insulation, it remains to be seen whether or not capillary forces are a factor. Attention will be given to measurement of a capillary rise coefficient in hopes of determining the role of surface tension forces in moisture migration through insulation.

It will be the aim of this investigation to determine if Darcy's Law or some other appropriate mathematical expression relating liquid flow to the driving forces can be established. Having identified such an expression would alter the form of the mathematical model proposed by Thomas, et al. for analyzing the heat and mass transfer mechanisms in wetted fiberglass insulation materials. Improvement in the accuracy of Thomas's computer model over a range of higher moisture concentrations should come as a direct result.

1.3 Objectives and Scope

The applicability of Darcy's Law and Whitaker's postulate for capillary flow to correlate liquid flow in fiberglass insulation is investigated. The investigation is primarily experimental with an emphasis on determining whether or not these general mathematical relationships for correlating flow apply with constant transport parameters such as hydraulic conductivity and the capillary rise coefficient. Specific objectives include developing an experimental procedure for measuring the hydraulic conductivity of fibrous materials, determination of hydraulic conductivities for ranges of fiberglass insulations, and investigating other flow parameters which are necessary to describe the flow of liquid water through fiberglass insulation materials.

The presentation that follows is organized into chapters. The experimental procedure and analysis are presented in the following

chapter. Chapter III is devoted to a presentation and discussion of the results of the investigation. Chapter IV contains conclusions of the study and recommendations for future work.

CHAPTER II

EXPERIMENTAL PROCEDURE AND ANALYSIS

The equations developed by Whitaker (19) to describe the drying of porous media appear to be most suitable for treating the bulk flow of liquid water in fiberglass insulation materials. It is assumed that the flow rates encountered in drying processes are of the same order of magnitude of those encountered in rooftop insulation. In a simplified form of Whitaker's equation for the bulk flow of liquid water, only two phenomenological parameters need be evaluated. In this section, an analysis of the equation of motion of liquid water through insulation is presented as well as a description of the experiments designed to isolate the different flow parameters encountered.

2.1 Analysis of the Equation of Motion

Whitaker (19) has developed an expression similar in form to

$$n_3''(z,t) = \frac{K\rho_3 V_3'''}{\mu_3} \left[\beta_3 \frac{\partial V_3'''}{\partial z} + \gamma_3 \frac{\partial T}{\partial z} + (\rho_3 - \rho_{12})g \right] \quad (8)$$

to describe the mass flux of liquid water through a porous material in a drying process in which the mechanisms governing flow depend entirely on gravity and surface tension forces. Equation 8 applies to flows where the liquid phase is continuous; that is, no isolated islands of water

exist throughout the insulation matrix. With the lack of published information regarding the numerical values of the flow parameters K, β_3, and γ_3 for insulation materials, it becomes necessary to experimentally determine these quantities and to determine if they are constant for a given insulation.

For the special case of n_3'' approaching zero (no flow), Eq. 8 reduces to

$$0 = \beta_3 \frac{\partial \Psi_3'''}{\partial z} + \gamma_3 \frac{\partial T}{\partial z} + (\rho_3 - \rho_{12})g. \tag{9}$$

The literature (20) suggests that even in the case of moderate temperature gradients, liquid flow attributed to such gradients is negligible. In the present investigation which considers only isothermal conditions, Eq. 9 reduces to

$$0 = \beta_3 \frac{\partial \Psi_3'''}{\partial z} + (\rho_3 - \rho_{12})g. \tag{10}$$

In this form, knowing values for ρ_3 and ρ_{12}, the capillary rise coefficient, β_3, can be calculated by experimentally determining the liquid moisture distribution in a column of insulation under 'no-flow' conditions.

In Eq. 8, K represents the insulation hydraulic conductivity. In determining K for the fiberglass insulations herein, this study was

concerned with saturated flows of an incompressible fluid through a homogeneous, nondeformable porous medium.

The parameters K and β_3 are expected to be different for different types of insulation. Whether or not these values are independent of the liquid flow rate and volume fraction of liquid water remains to be determined. Two different experimental set-ups were designed to effectively isolate the flow parameters for measurement.

2.2 Description of Apparatus for Measuring Hydraulic Conductivity

The experimental apparatus used to determine K for the insulations in this investigation is pictured in Fig. 3, and will be referred to as the hydraulic conductivity (HC) chamber. The HC chamber consisted of a hollow plexiglas square tube with a 0.2 m x 0.2 m cross-section and one meter high. The chamber was open at the top end and fitted with a valve at the bottom end. This valve allowed the tube to be emptied between experiments. Four pressure taps were drilled along the height of the tube, each 50.8 mm apart. Pressure measurements were made by connecting the pressure taps to a bank of open manometer tubes via flexible Tygon^R tubing. Two 13 mm overflow holes were drilled at the top of the tube.

The HC chamber was part of a recirculating system, pictured in Fig. 4 and shown schematically in Fig. 5. The other system components consisted of a 1/3 HP recirculating pump, a rotameter calibrated for flow rate measurement, a throttle valve designed to regulate the flow rate, and a holding tank which acted as a reservoir into which the system could be originally filled. Distilled water was chosen over

Figure 3. View of HC Chamber.

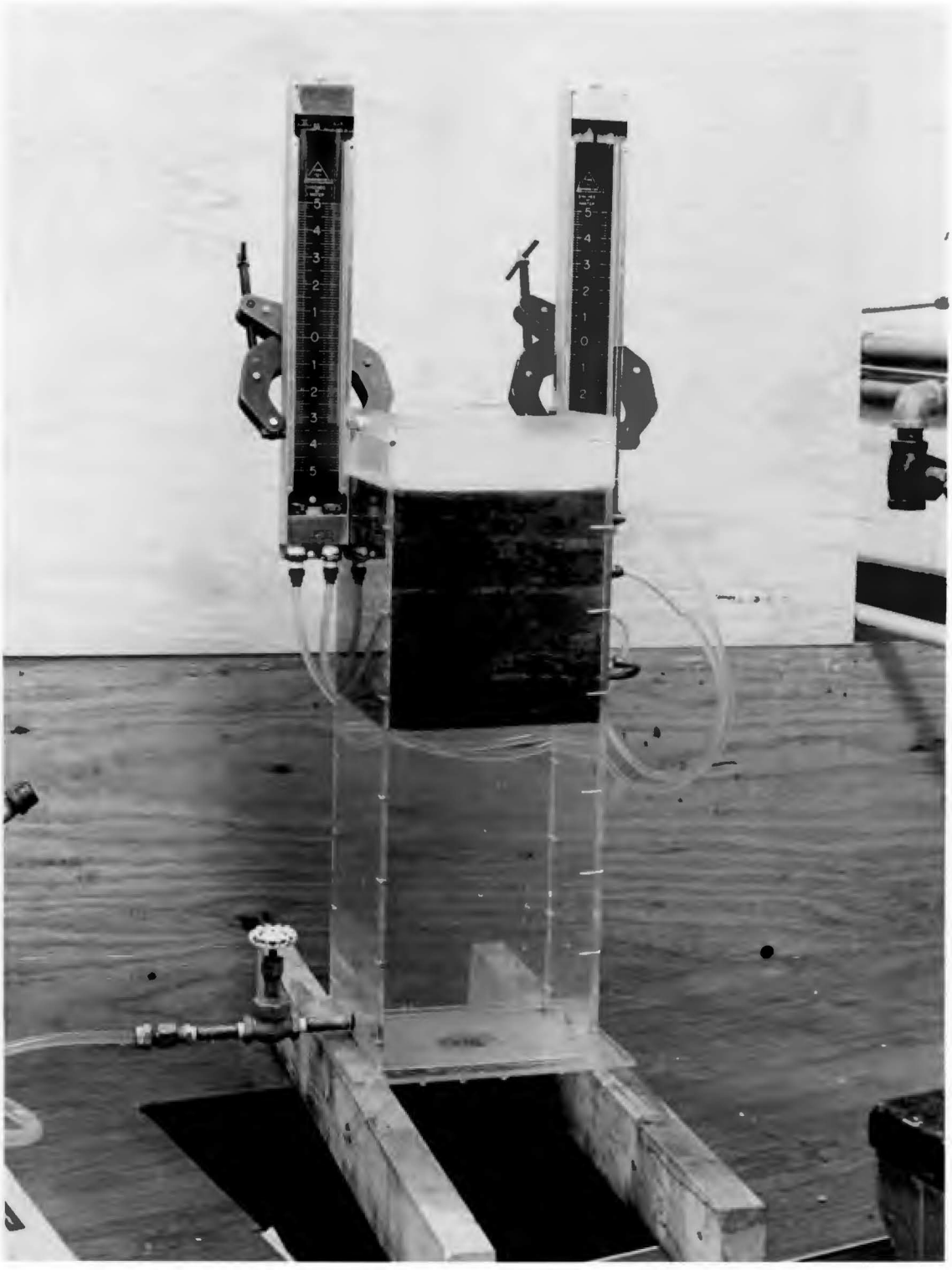

Figure 4. Overall View of Recirculating System.

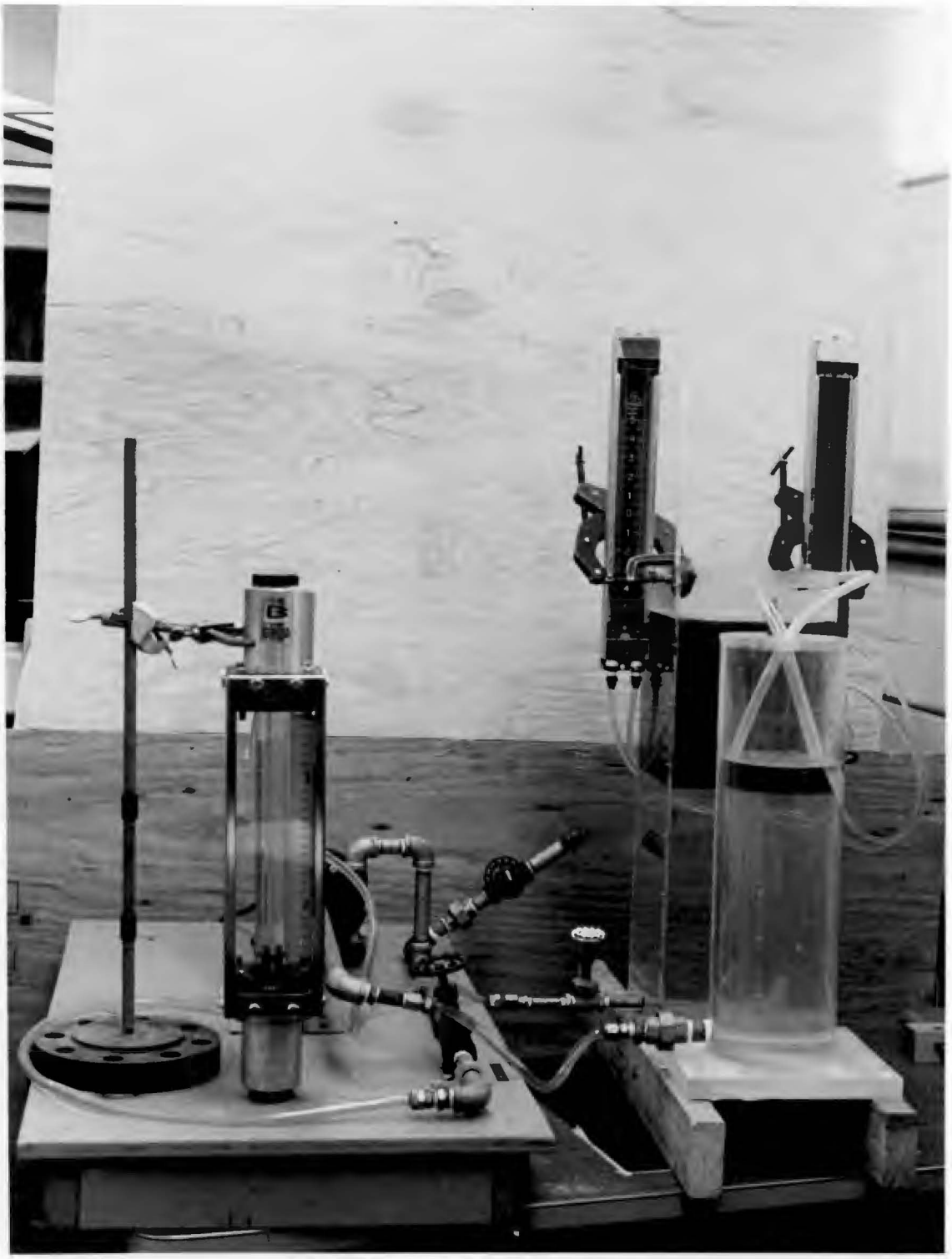

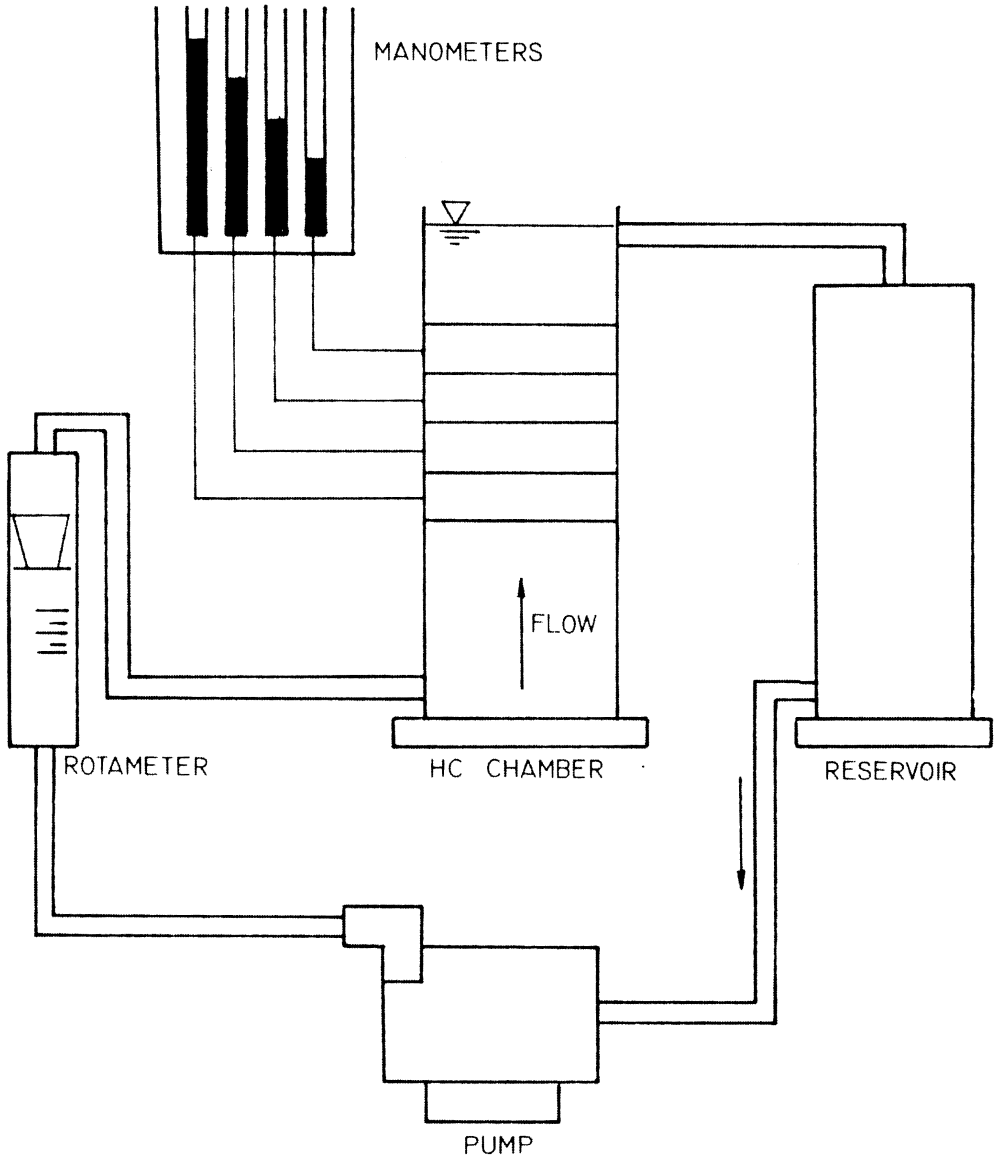

Figure 5. Schematic of Recirculating System.

ordinary tap water as the working fluid because use of the latter resulted in entrapment of air bubbles within the fiberglass insulation. The evolution of gases dissolved in the tap water would cause small air bubbles to become trapped in the pores of the insulation, resulting in an apparent decrease in the hydraulic conductivity value over time. A thermometer was submerged in the HC chamber for purposes of monitoring temperatures for density and viscosity determination, which were obtained from standard tables.

The original set-up was configured to have the liquid flow downward under its own weight which is more nearly like the application encountered. This attempt was unsuccessful because it was not possible to completely eliminate the problem with air build up below the sample, which partially blocked the flow.

2.3 Test Procedure for Measuring K

In preparation for an experimental run, a number of snugly fitting 50 mm thick insulation samples were inserted into the tube so that no air space remained between adjacent pieces or between the insulation and the walls of the tube. Water was introduced at the bottom of the tube, and when the level of the water approached the lowest piece of insulation, the flow rate was reduced greatly to allow the advancing water front to evenly and fully saturate the insulation. Once the water level reached the overflow holes, flexible tubing directed the water into the holding tank for recirculation. Pressure drops were recorded for a

number of different flow rates to determine whether K was flow dependent or remained constant for different flow rates.

Based on the experience gained in this investigation, a recommended test procedure for measuring hydraulic conductivities of fiberglass insulation with the apparatus used in this investigation is outlined in Appendix A.

2.4 Description of Apparatus for Measuring Capillary Rise Coefficient

The capillary rise coefficient, β_3, in Eq. 8 was measured experimentally using the apparatus pictured in Fig. 6. A schematic of the system appears in Fig. 7. The apparatus consisted of a hollow right circular cylindrical tube, constructed of plexiglass and measuring one meter high with a 165 mm inside diameter, and hereafter referred to as the capillary rise chamber. A 6 mm diameter hole was drilled near the bottom of the chamber from which water could enter via flexible plastic tubing. The water level inside the chamber was controlled externally by a constant level reservoir which was supplied by a continuous source of tap water. The relative humidity inside the capillary rise chamber was monitored using wet bulb and dry bulb thermometers.

2.5 Test Procedure for Measuring Capillary Rise Coefficient

In preparation for an experimental run, a number of 150 mm diameter circular slabs of insulation of varying thicknesses were first dried, weighed, and then placed in a wire framework, designed to align the individual pieces. This framework was lowered inside the capillary rise

Figure 6. Overall View of Capillary Rise System.

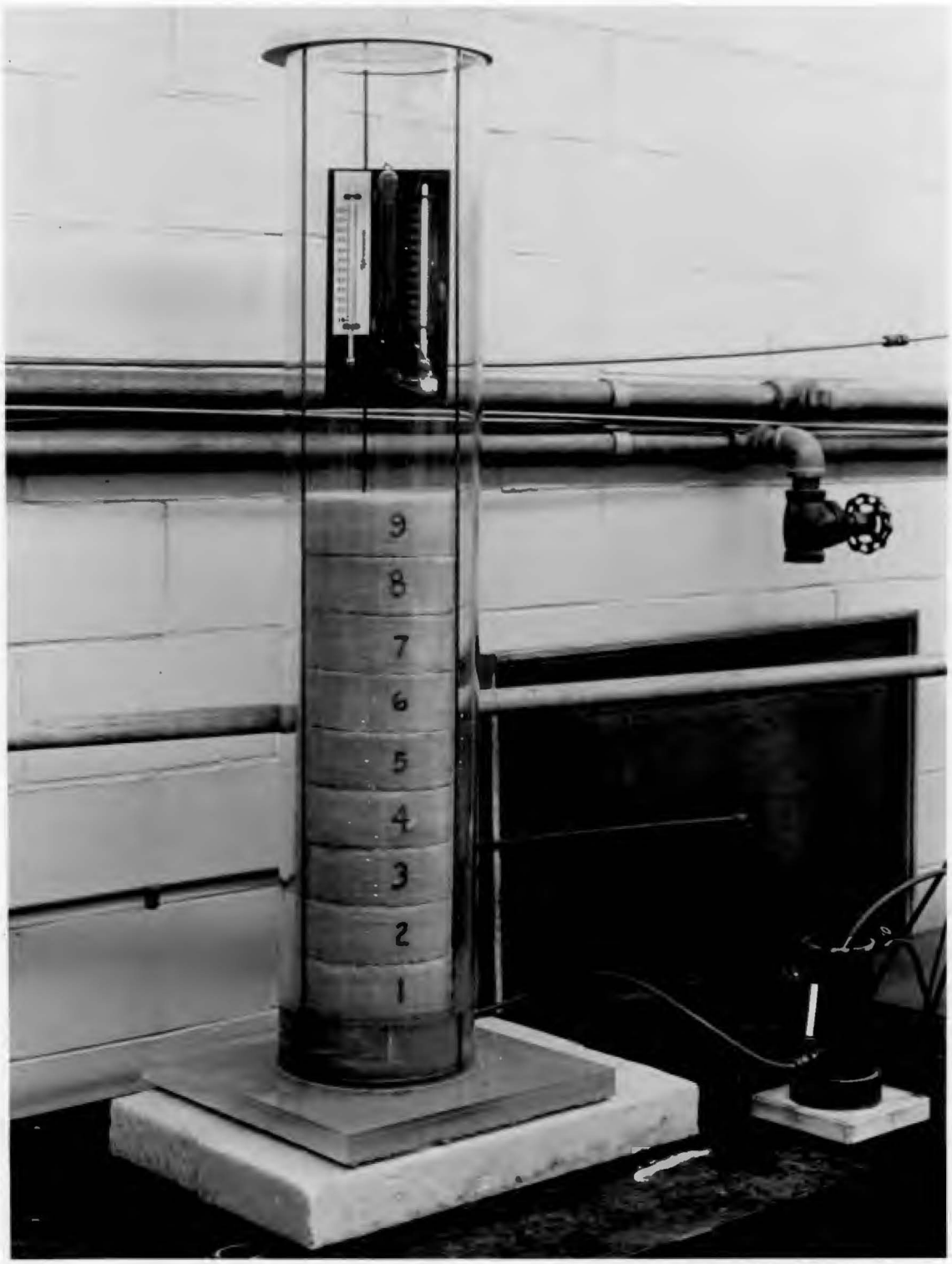
9
8
7
6
5
4
3
2
1

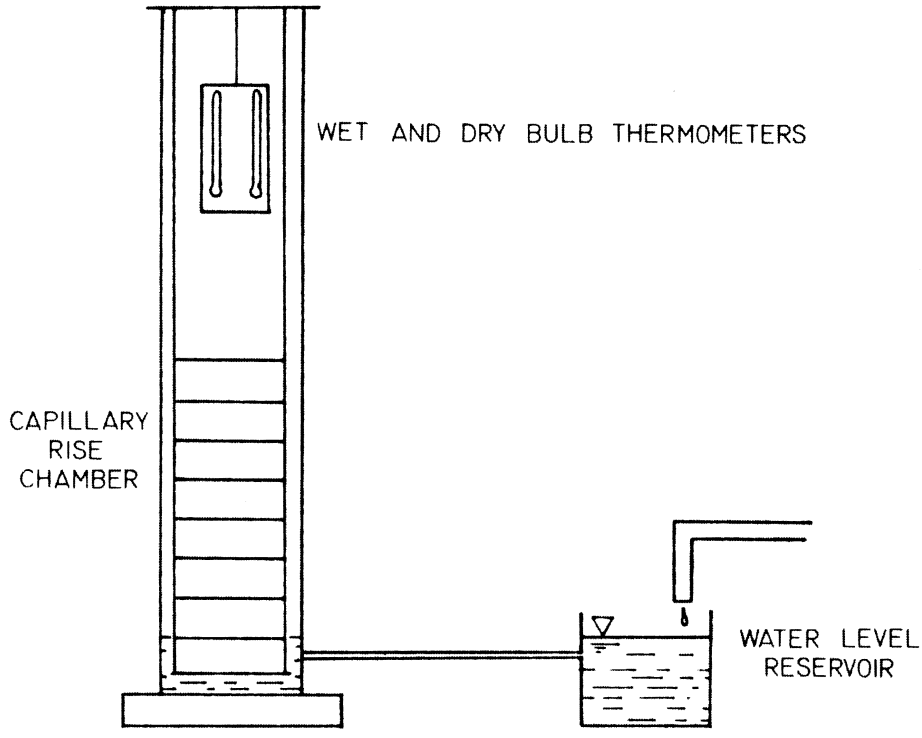

Figure 7. Schematic of Capillary Rise System.

chamber. As the water began to 'wick up' the column of insulation, the water level in the reservoir was maintained to just submerge the lowest slab of insulation. This procedure helped to improve the wettability at the insulation-water interface. Consequently, any moisture gain above the bottommost slab resulted from capillary action (or moisture transfer in the vapor phase discussed in a later section). A cover was placed over the top of the chamber to prevent evaporation of the water source and to create an inside environment as close as possible to 100 per cent relative humidity.

The samples were removed periodically and weighed using a Fischer^{R} Gram-atic balance, accurate to within $\pm$ 0.001 g. Once equilibrium was achieved, the moisture gradient term, based on finite slab thicknesses, could be experimentally quantified. The equilibrium condition was indicated by a less than 0.025 per cent change in mass between any two consecutive weighings of the slab at the head of the advancing water front.

A number of experimental runs was conducted for each of the insulations to ensure repeatable and reliable results.

CHAPTER III

RESULTS AND DISCUSSION

The equation of motion for liquid water through porous media in the drying state proposed by Whitaker expresses the bulk flow of water as the sum of terms representing surface tension and gravitational forces. Based on the analysis presented in the previous chapter, it was shown that the liquid flow process can be modeled provided two phenomenological parameters are experimentally determined. The results of the experiments designed to determine the applicability of Eq. 8 and values for these parameters are presented in this chapter.

3.1 Hydraulic Conductivity

In order to be confident of the accuracy of the apparatus designed to measure hydraulic conductivities in this investigation, the apparatus was cross-checked by measuring the pressure drop across a bed of glass spheres packed within the test section. Glass spheres were used as the test medium because literature regarding a reference for hydraulic conductivity values of porous materials could not be found. Tests over a range of flow rates were made. By comparing the measured pressure drops with those predicted by two sources widely quoted in the literature, it was shown that the instrument operated satisfactorily within the bounds proposed by the correlations of Carman (4) and Ergun (9). Results of this exercise are presented in Fig. 8. A description of the

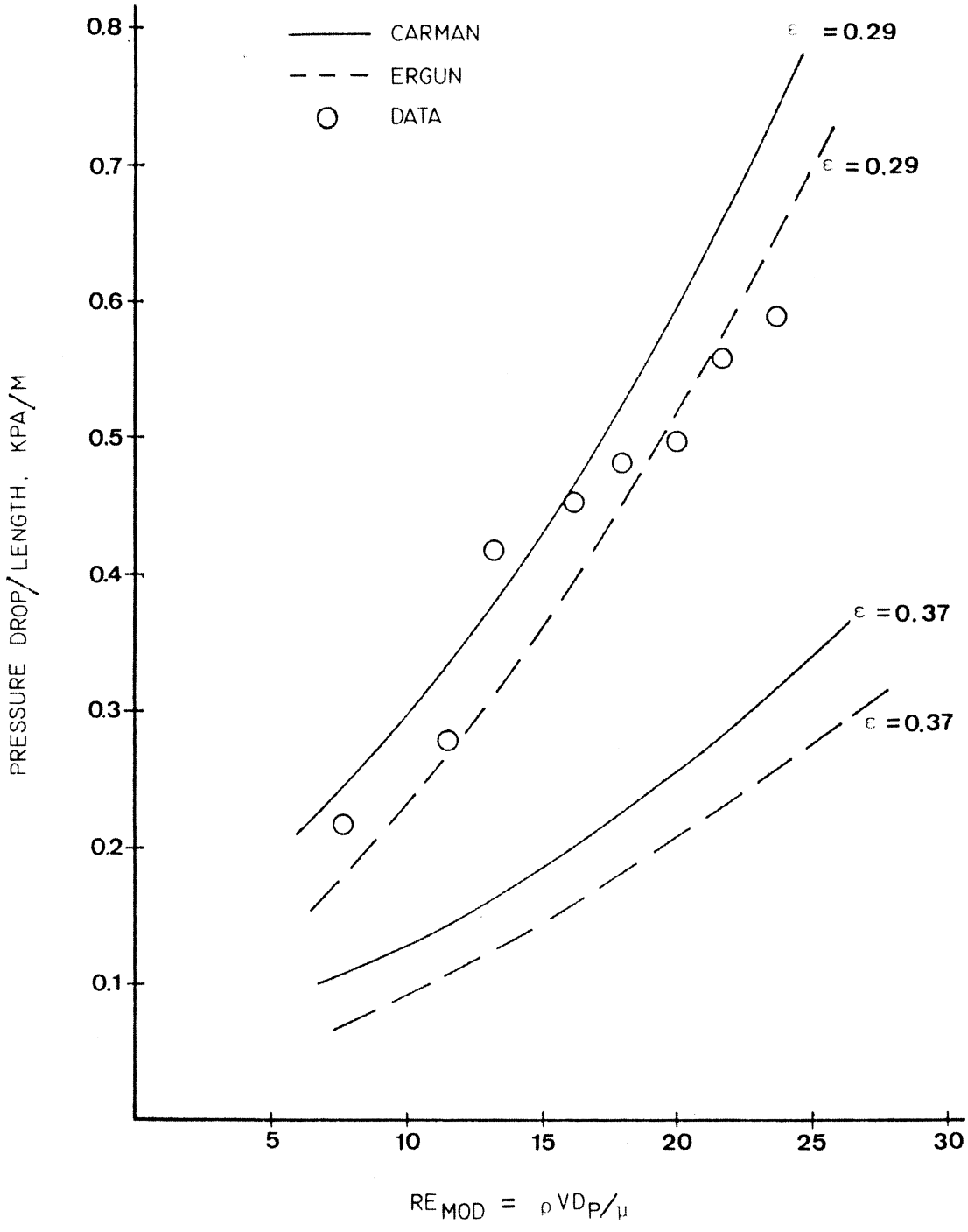

Figure 8. Pressure Drop through a Packed Bed of Glass Spheres.

cross-check exercise together with an explanation of the details of Fig. 8 are given in Appendix B.

A regime of flow wherein water migrates under the force of its own weight was created in this investigation by adjusting the flow rate in the system until the pressure drop per unit length across a given sample was equal to $\rho_3 g$. This condition was denoted by a difference in water levels in any two adjacent manometer tubes equal to the distance between the two corresponding pressure taps. The mass fluxes measured in this investigation range from 1.0 to 6.0 kg/s-m^2. These fluxes were found to be of the same order of magnitude of those encountered in the regime of water flowing under its own weight.

The measured pressure drops through the insulations tested were determined using the procedure described in Chapter II. Each of the three types of insulation was tested six times. (Three different samples of each insulation were tested, and a duplicate run was made each time to ensure experimental repeatability.) The data collected from measuring the pressure drop across a sample of insulation C over mass fluxes from 1.22 kg/s-m^2 to 5.27 kg/s-m^2 are given in Table 2. The experimental data points of Table 2 are plotted in Fig. 9, together with a curve representing Iberall's fiber theory correlation (15).

As can be clearly seen from Fig. 9, the data shows a linear relationship between flow rate and pressure drop. The results agree closely with Darcy's Law but not with Iberall's fiber theory. The latter theory predicts pressure drops up to 46 per cent different from those

Table 2. Pressure Drop through Insulation C. Sample 8.

Temp, T (C)	Density, ρ (kg/m^3)	Viscosity, μ (kg/m-s)	Mass Flow Rate, $\dot{m}$ (kg/s)	Pressure Drop, $\Delta p/L$ (kPa/m)
17	998.9	1.081×10^{-3}	0.0460	2.45
17	998.9	1.081×10^{-3}	0.0808	3.59
17.5	998.8	1.067×10^{-3}	0.1111	4.90
17.5	998.8	1.067×10^{-3}	0.1430	6.21
17.5	998.8	1.067×10^{-3}	0.1690	7.35
18	998.7	1.053×10^{-3}	0.1994	9.06
18	998.7	1.053×10^{-3}	0.0547	2.37
18	998.7	1.053×10^{-3}	0.0706	3.02
18	998.7	1.053×10^{-3}	0.1010	4.25
18	998.7	1.053×10^{-3}	0.1300	5.31
18	998.7	1.053×10^{-3}	0.1574	6.37
18	998.7	1.053×10^{-3}	0.1864	7.35

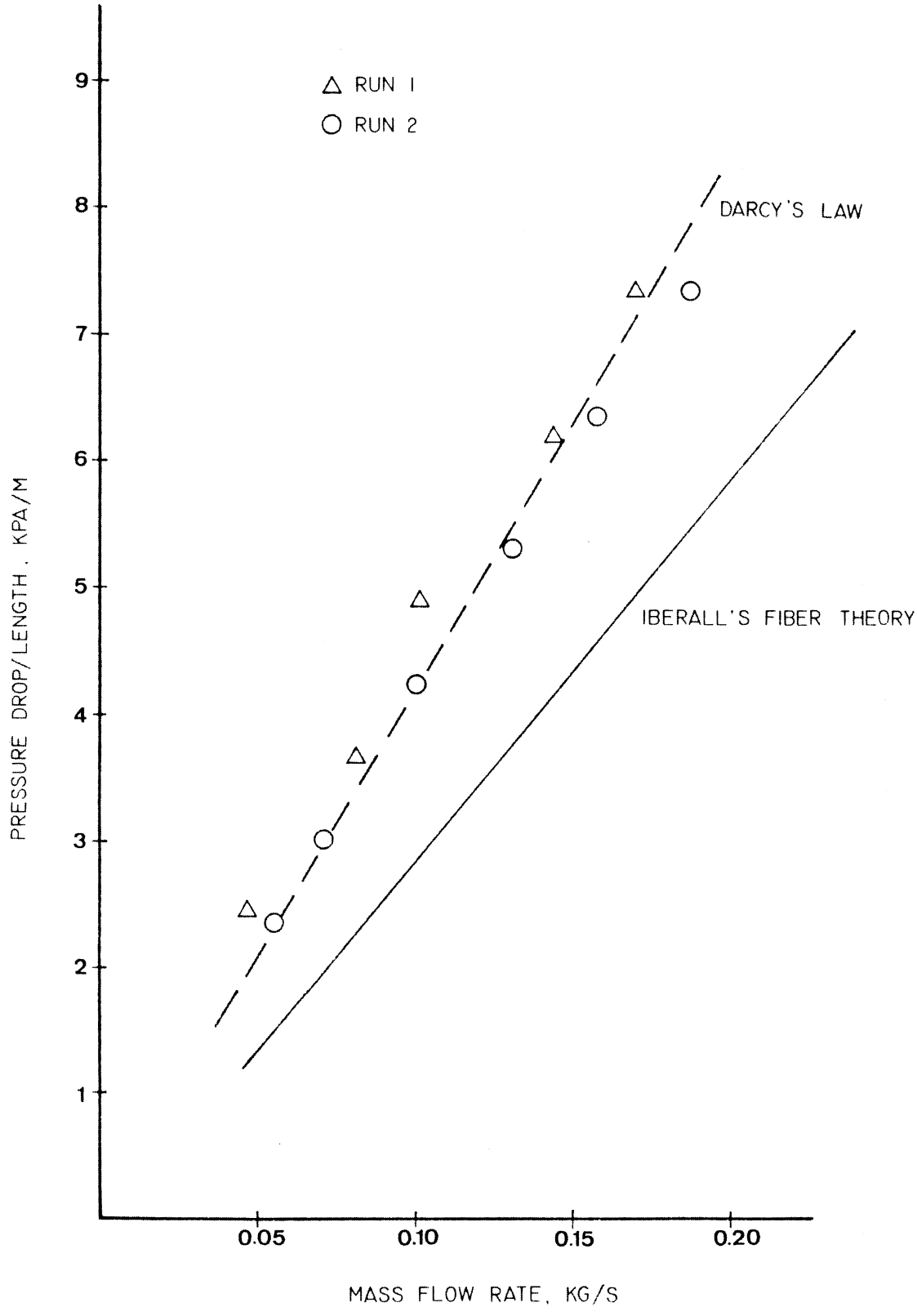

Figure 9. Pressure Drop through Insulation C.

experimentally determined. The correlations offered by Beavers and Sparrow (8) for non-Darcy flow through fibrous porous media do not apply to the regime of flow examined within. Furthermore, inertial effects are negligible for the range of flows involved in these experiments.

Similar pressure drop results for experimental runs involving insulations A and B are given in Tables 3 and 4. The data is plotted in Figs. 10 and 11. Again, the results show a strong linear relationship between the pressure drop through a column of insulation and the flow rate which passes through it. A complete set of pressure drop data for all other experimental runs is presented in Appendix C.

For materials that follow Darcy's Law, the hydraulic conductivity can be determined from

$$K = \frac{-\mu V}{(\Delta p/L)} \cdot \qquad (11)$$

Equation 11 was solved for each of the cases investigated and the dashed lines in Figs. 9, 10, and 11 graphically depict equations of the form $\Delta p/Lm = \mu/\rho AK$, where the K-value used in the denominator is an average value taken from Table 5, which also lists other pertinent statistical parameters. While no correlation was made between the measured K-values and densities for the same sample of insulation, the range in K-values is assumed to be attributed to product variability. For all the samples tested, no correlation between flow rate and hydraulic conductivity was found. This observation would tend to confirm

Table 3. Pressure Drop through Insulation A. Sample 2.

Temp, T (C)	Density, ρ (kg/m^3)	Viscosity, μ (kg/m-s)	Mass Flow Rate, $\dot{m}$ (kg/s)	Pressure Drop, $\Delta p/L$ (kPa/m)
22	997.9	9.548×10^{-4}	0.0547	2.45
22	997.9	9.548×10^{-4}	0.0792	3.51
22	997.9	9.548×10^{-4}	0.1082	4.65
22	997.9	9.548×10^{-4}	0.1371	5.79
22	997.9	9.548×10^{-4}	0.1631	6.77
22	997.9	9.548×10^{-4}	0.1862	7.83
22	997.9	9.548×10^{-4}	0.2079	8.46
21	998.1	9.784×10^{-4}	0.0547	2.61
21	998.1	9.784×10^{-4}	0.0821	3.83
21	998.1	9.784×10^{-4}	0.1140	5.47
21	998.1	9.784×10^{-4}	0.1487	6.77
21	998.1	9.784×10^{-4}	0.1704	7.67
21	998.1	9.784×10^{-4}	0.2022	9.39

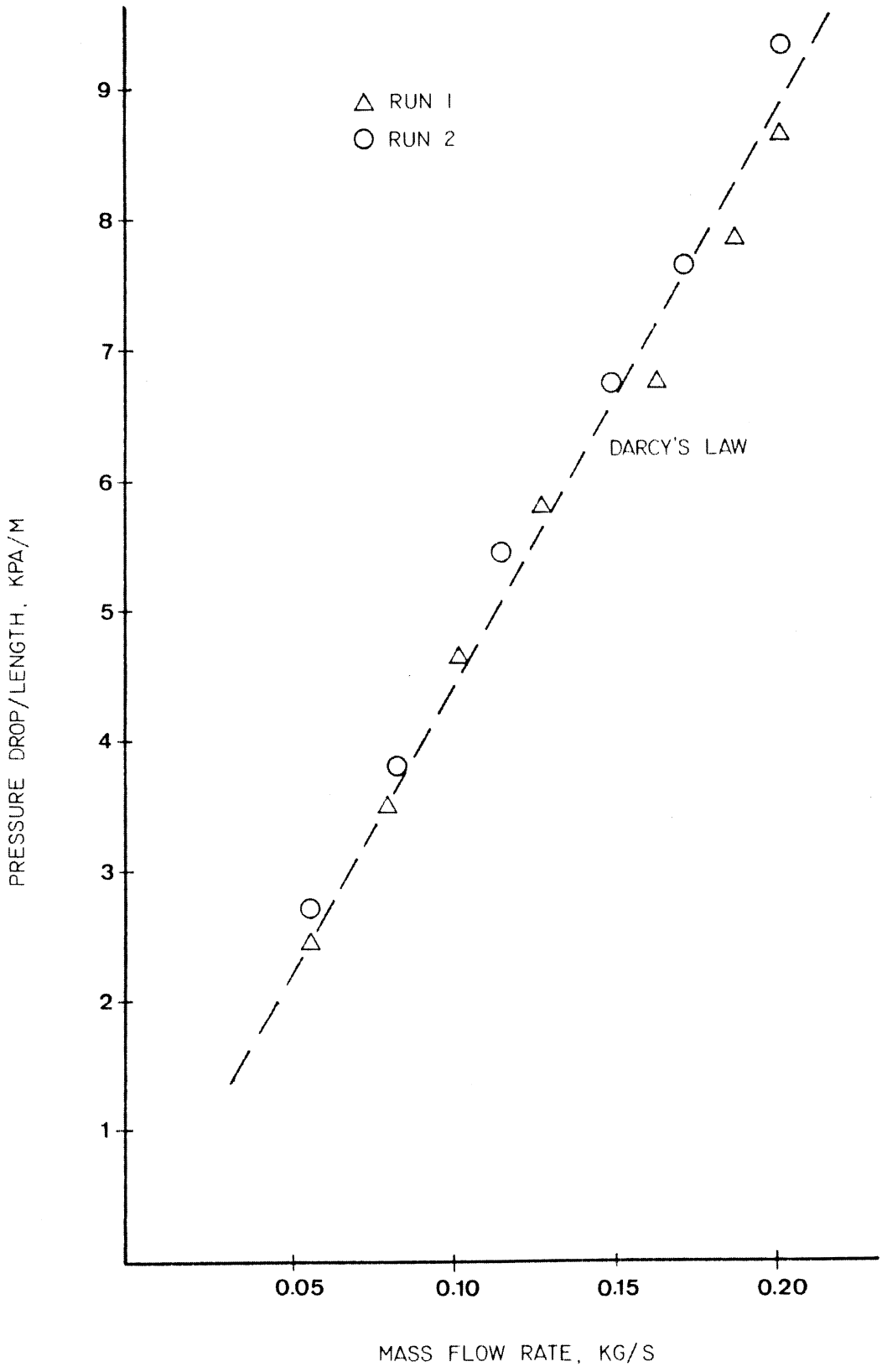

Figure 10. Pressure Drop through Insulation A.

Table 4. Pressure Drop through Insulation B. Sample 4.

Temp, T (C)	Density, ρ (kg/m^3)	Viscosity, μ (kg/m-s)	Mass Flow Rate, $\dot{m}$ (kg/s)	Pressure Drop, $\Delta p/L$ (kPa/m)
22	997.9	9.548×10^{-4}	0.0821	2.78
22	997.9	9.548×10^{-4}	0.1067	3.51
22	997.9	9.548×10^{-4}	0.1356	4.41
22.5	997.8	9.439×10^{-4}	0.1616	5.22
23	997.6	9.330×10^{-4}	0.1789	5.71
23	997.6	9.330×10^{-4}	0.2079	6.52
18	998.7	1.053×10^{-3}	0.0894	3.35
18	998.7	1.053×10^{-3}	0.1155	4.25
18	998.7	1.053×10^{-3}	0.1430	5.14
18	998.7	1.053×10^{-3}	0.1661	5.80
18.5	998.6	1.041×10^{-3}	0.1893	6.61
19	998.5	9.330×10^{-3}	0.2109	7.10

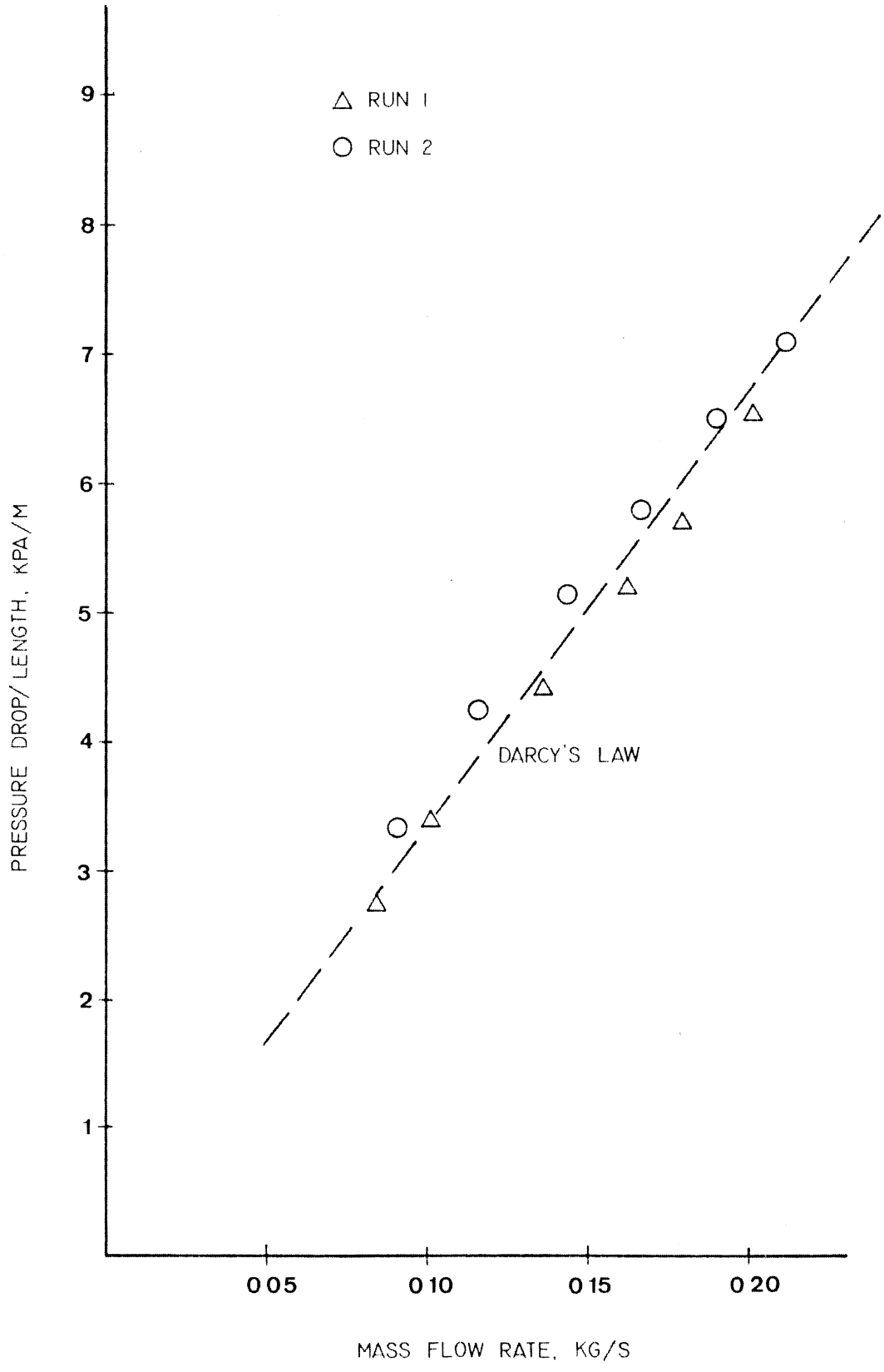

Figure 11. Pressure Drop through Insulation B.

Table 5. Hydraulic Conductivity of Insulations Tested.

Insulation	Average K-value* ($m^2 \times 10^{-10}$)	Standard Deviation ($m^2 \times 10^{-10}$)	95% Confidence Interval ($m^2 \times 10^{-10}$)
A	5.05	0.47	4.90 - 5.20
B	8.42	0.63	8.21 - 8.63
C	6.55	0.22	6.48 - 6.62

*Based on thirty-six tests

that K is independent of the other flow parameters but is naturally dependent on the particular sample.

One area of concern regarding the results of the hydraulic conductivity measurements reported is the fact that the least dense insulation tested (insulation A) has the lowest K-value and thus presents a greater obstruction to flow than either of the heavier insulations. This result seems to be in contrast with what one would normally expect. On the other hand, insulation C has a K-value lower than insulation B, which supports the notion that the more dense an insulation is, the less conductive it would be to a fluid flowing through it. In an effort to explain these unexpected results, attention was given to fiber diameter measurements made from the scanning electron microscope photomicrographs (Fig. 1). Preliminary attempts to explain this effect by a simplified model based on flow over staggered banks of tubes were unsuccessful (see Appendix D). Further investigation of this effect was beyond the scope of the present investigation.

3.2 Moisture Distribution

The apparatus designed to measure the capillary rise coefficient, β_3, was originally built based on preliminary data that suggested capillary forces in a drying process may be strong enough to cause liquid water to migrate up a column of insulation as far as one meter. Later careful analyses of experimental data showed that the maximum capillary rise for all three insulations studied was not actually

greater than about 13 mm. While moisture gain above 13 mm was observed in the samples, this gain was later attributed to moisture transfer in the vapor state. Inability to detect moisture distributions along such a small height prevents an accurate determination of the parameter β_3. This result suggests that the contribution of surface tension forces to the migration of liquid water in fiberglass insulation is negligible.

Preliminary investigations into the role of surface tension forces in the flow problem, following the procedures outlined in Chapter II, showed that slabs of insulation at heights as far as 0.4 m had a measurable net mass gain during the course of experiments run over a period of three weeks. In addition, measurements showed evidence that the water front was still advancing after this time period, indicating that 'no-flow' conditions may take an extremely long time to achieve. Figure 12 shows a moisture distribution curve for insulation A after time intervals up to three weeks. While a gentle increase in moisture content is seen nearer the water source, close inspection of these results revealed that the net mass gain of all slabs, except the bottom-most one, was of an extremely small order of magnitude. The change in mass of these slabs was deemed so small that some means of mass gain other than by capillary transport could be playing a factor.

In order to test this theory, a simple experiment was designed wherein an impermeable stainless steel plate, acting as a barrier to liquid water transport, was placed between the submerged base slab of insulation and the rest of the insulation stack. Except for the bottom-most 13 mm slab, the mass gains measured for the slabs were remarkably

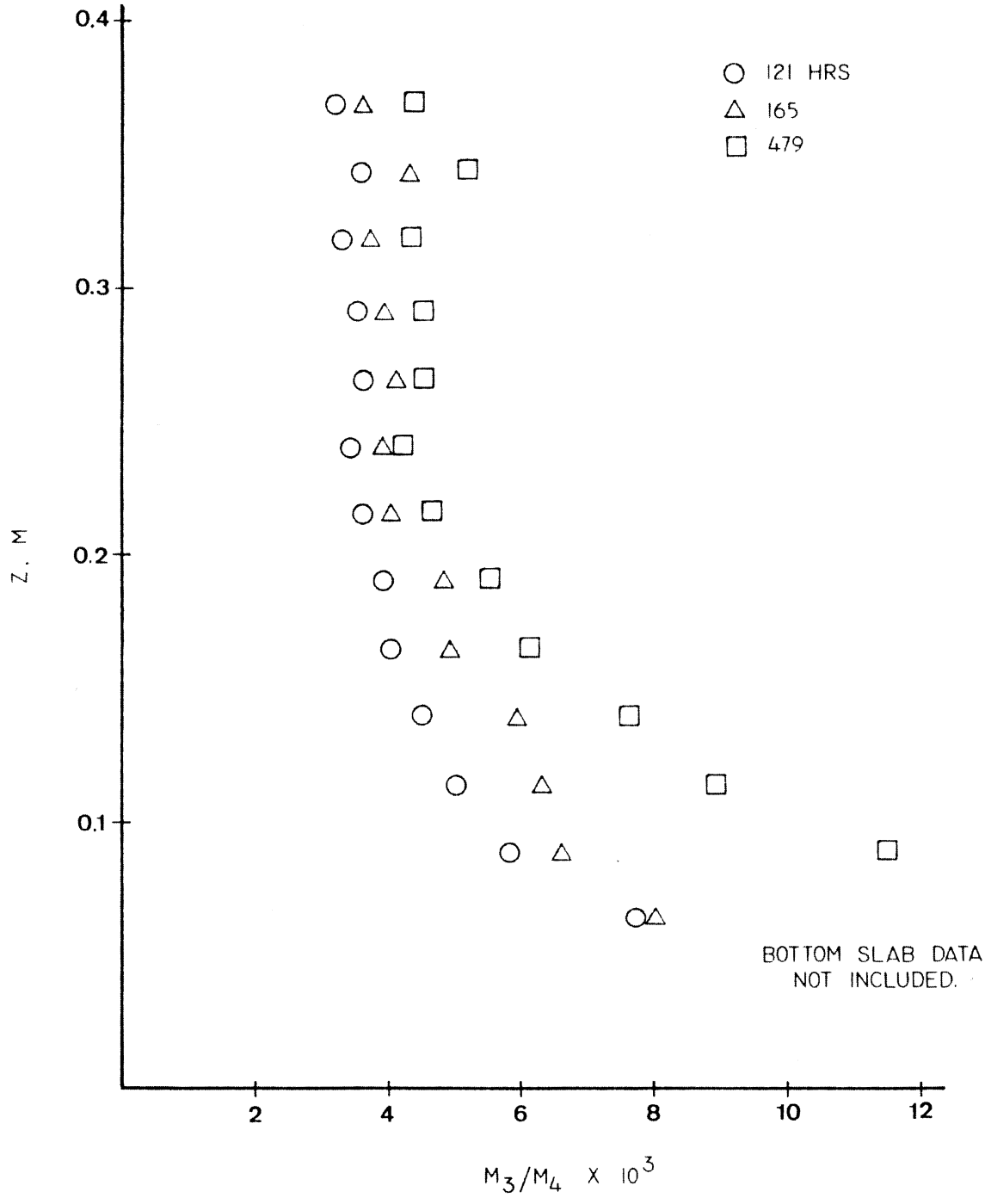

Figure 12. Moisture Distribution Curve. Insulation A.

similar to those measured when no barrier was used at all. Figure 13 illustrates this finding for a sample of insulation B slabs run for a period of forty hours. Similar results exist for insulations A and C, as shown in Figs. 14 and 15.

The mass gains reported can not be accounted for by changes in the relative humidity or ambient temperature of the voids within the insulation. An increase in the relative humidity of the air/water vapor mixture occupying the voids of the insulation would result in a net mass loss. The mass gain could be attributed to the migration of water in the vapor phase. Other explanations for this phenomenon were entertained, however a suitable conclusion regarding the mass gain phenomenon was not determined.

Considering the relative magnitude of the mass gain experienced by the bottommost slab when compared to the mass gains of all other slabs, a typical moisture distribution curve for any of the insulations studied would appear like the one shown in Fig. 16.

These results show that the role of capillary forces in describing the movement of liquid water up columns of all of the insulations studied in this investigation is significant only in a small region adjacent to the water source. Within the measurement capabilities of the capillary rise experiments conducted herein, it has been shown that water rises no higher than 13 mm up a column of insulation when put in contact with a continuous source. Because of the characteristics of the insulation studied, samples much less than 13 mm thick can not be cut. More accurate means of moisture detection other than available for these

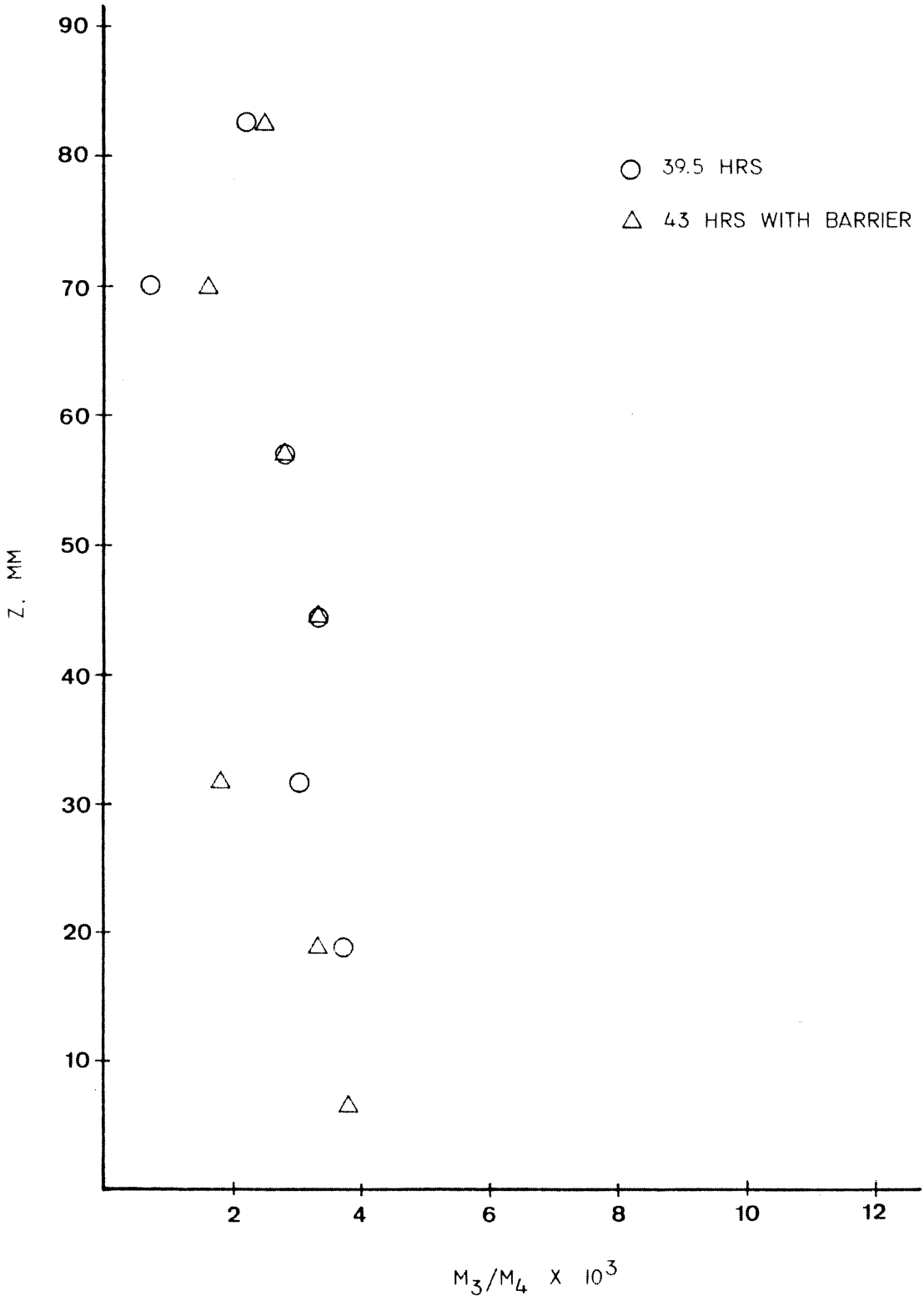

Figure 13. Moisture Distribution with Barrier, Insulation B.

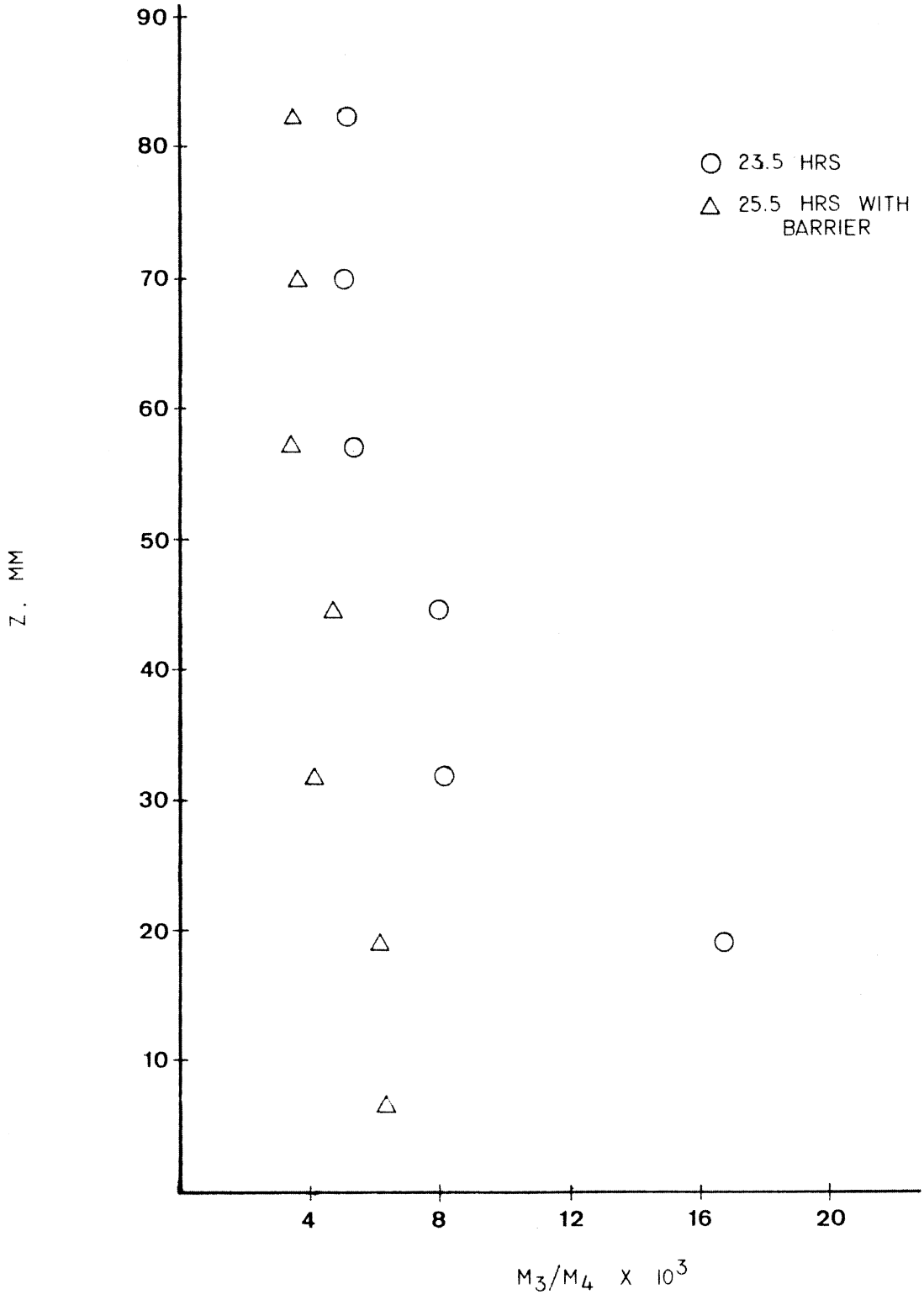

Figure 14. Moisture Distribution with Barrier, Insulation A.

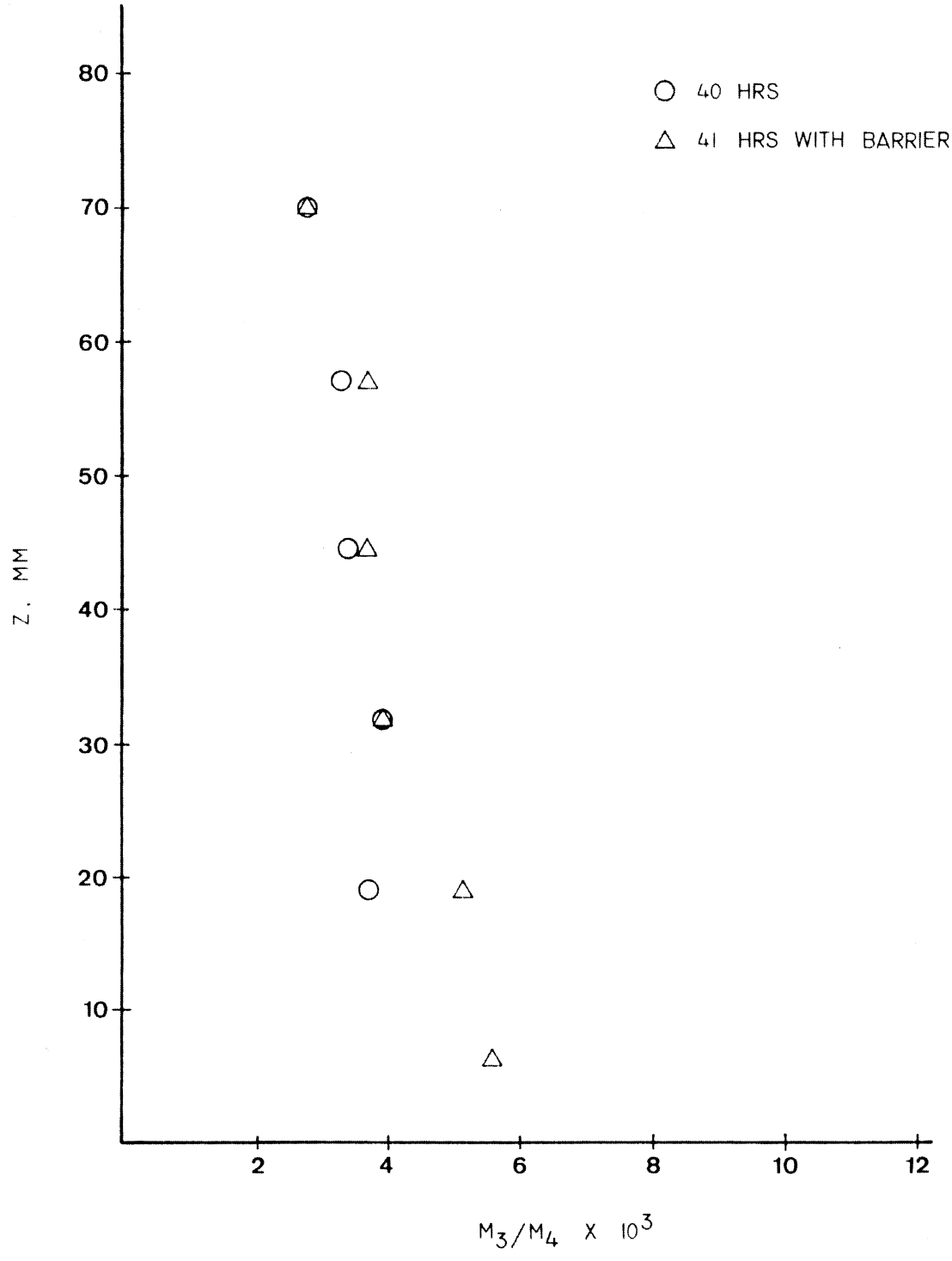

Figure 15. Moisture Distribution with Barrier, Insulation C.

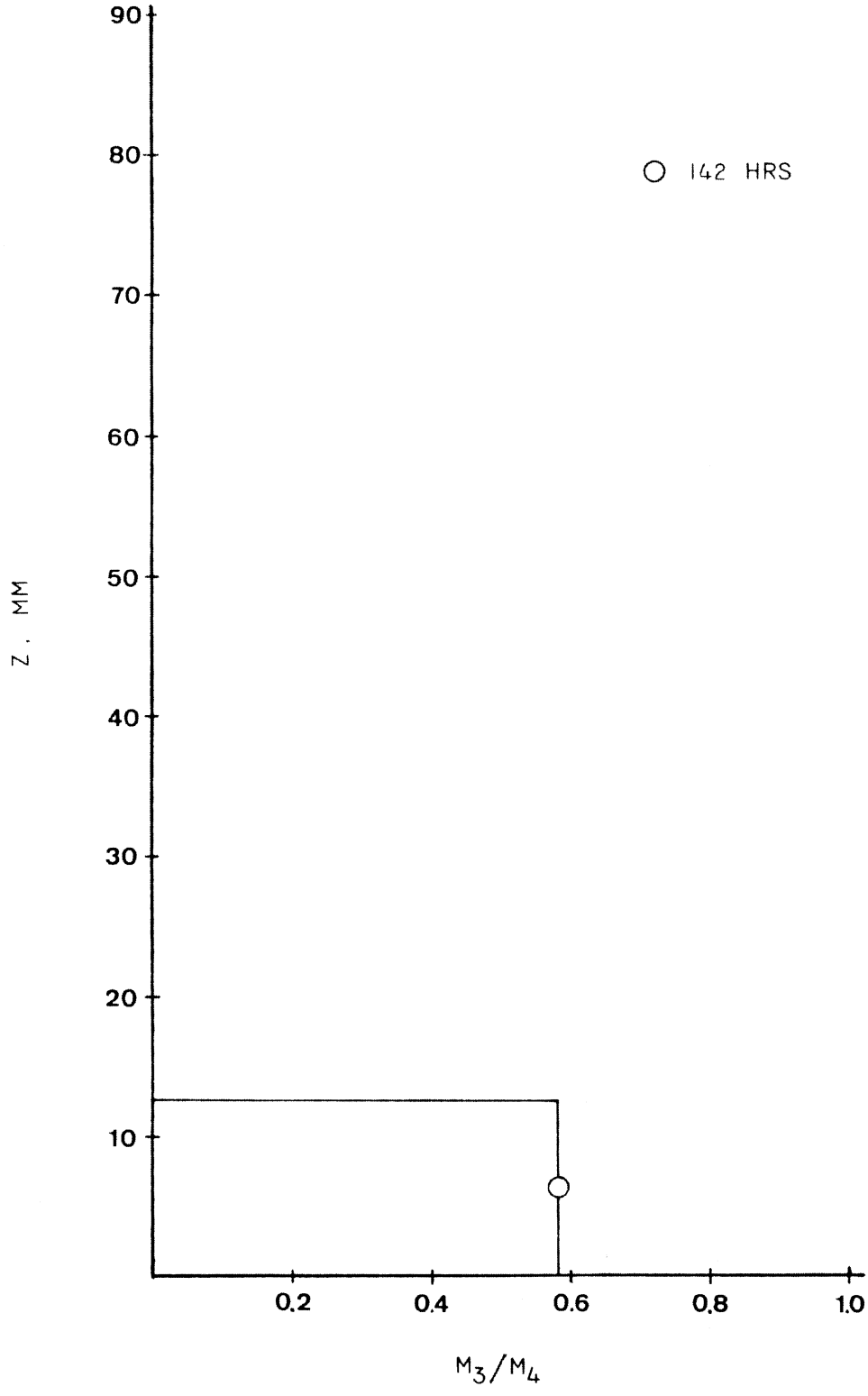

Figure 16. Typical Moisture Distribution Curve, Insulation B.

experiments would be necessary to determine the moisture distribution along a 13 mm height of insulation. Within the measurement capabilities available in this investigation, the role of capillary forces in the migration of water up a column of fiberglass insulation materials is insignificant.

The inability to measure the capillary rise coefficient, β_3, suggests the need for alternative experimental procedures. An experiment whereby water is allowed to drain from an initially saturated column of insulation as opposed to being imbibed through an initially dry column (as was done in this investigation) may provide valuable information. Any hysteresis effects present in capillary flow processes could be detected through such an experiment.

3.3 Moisture Migration in Fiberglass Insulation

Having shown that capillary forces are negligible in determining liquid migration in fiberglass insulation materials, Eq. 8 by Whitaker reduces to

$$n_3''(z,t) = \frac{-K\rho_3 \forall_3'''}{\mu_3} (\rho_3 - \rho_{12})g \ , \qquad (12)$$

where the term containing β_3 and representing flow attributed to surface tension forces has been dropped. According to the experiments conducted in this investigation, Eq. 12 gives a complete description of the flow process involved in the migration of liquid water through fiberglass insulation. Experimental determination of the hydraulic conductivity

term, K, and a measurement of the volume fraction of water, at least under saturated conditions, is all that is needed to permit a quantitative analysis of the equation of motion of liquid water.

It should be noted that in the case of a saturated sample of insulation in which water flows under the force of its own weight, the following conditions apply:

$$\forall_3''' = 1$$

$$\rho_1 = \rho_2 = 0$$

$$\Delta p/L = \rho_3 g.$$

Making these substitutions, Eq. 12 becomes

$$n_3'' = \frac{\rho_3 Q}{A} = \frac{-K\rho_3}{\mu_3} \frac{\Delta p}{L} \quad . \tag{13}$$

Upon rearranging terms and simplifying, Eq. 13 becomes

$$Q = \frac{-KA}{\mu} \quad \frac{\Delta p}{L} \quad , \tag{14}$$

which is Darcy's Law.

CHAPTER IV

CONCLUSIONS AND RECOMMENDATIONS

An investigation was made to determine a mathematical model governing the flow of liquid moisture in fiberglass insulation materials. The aim of this study was to determine the applicability of proposed relationships between liquid flow and driving forces and to measure material flow parameters as required in the governing equation. Experiments were designed and carried out to measure these flow parameters and to determine the applicability of the mathematical model. The results in this investigation support the following conclusions:

1. Capillary forces, originally thought to make a significant contribution to the flow of liquid water in fiberglass insulation materials (ranging in densities from 50-120 kg/m^3), are negligible. Within the measurement capabilities available in this investigation, it was shown that water flow up a column of insulation put in contact with a continuous source of water measured no higher than 13 mm. While capillary action may be important in maintaining water in a pendular state with the matrix material, the bulk movement of liquid as a result of capillary pressure is insignificant.
2. In saturated flows through fiberglass insulation in which liquid water migrates under the force of its own weight, Darcy's Law

accurately describes the flow mechanism. The hydraulic conductivity, a constant material property for insulations ranging in density from 50 to 120 kg/m^3 and over a range of mass fluxes from 1.0 to 6.0 $kg/s\text{-}m^2$, is the only flow parameter which has to be experimentally determined in order to describe the motion of liquid water in fiberglass insulation.

Based on the research conducted in this investigation, recommendations for further work in studying the migration of moisture in insulation are as follows:

1. Further investigations should be made to relate hydraulic conductivity to the other physical properties of fiberglass insulation -- fiber diameter, porosity, and bulk density. This correlation would eliminate the need to experimentally determine the K-value for each different insulation of interest. The development of such a correlation should, of course, explain the unexpected results in the present investigation as related to a lack of correlation between the hydraulic conductivity and density of the insulation.
2. While the effective capillary action has been shown to be unimportant in the liquid migration process, further studies are in order to determine its role in unsaturated flow. The discovery of a threshold moisture fraction where correlation of liquid flow through the medium could be modeled with a Darcian expression would

aid in a better understanding of the contribution of capillary action to the overall problem.

REFERENCES

1. Bal, G. P., "Analysis of Heat Transfer and Moisture Distribution in Wetted Fiberglass Insulation Materials," Ph.D. Thesis, Virginia Polytechnic Institute and State University, August, 1980.

2. Huang, C. L. D., Siang, H. H., and Best, C. H., "Heat and Moisture Transfer in Concrete Slabs," Int. Journal of Heat and Mass Transfer, Vol. 22, 1979, pp. 257-266.

3. Luikov, A. V., "Systems of Differential Equations of Heat and Mass Transfer in Capillary-Porous Bodies (A Review)," Int. Journal of Heat and Mass Transfer, Vol. 18, 1975, pp. 1-14.

4. Thomas, W. C., Bal, G. P., and Onega, R. J., "Heat and Moisture Transfer in a Glass Fiber Roof-insulating Material," Thermal Insulation, Materials, and Systems for Energy Conservation in the '80s, ASTM STP 789, F. A. Govan, D. M. Greason, and J. D. McAllister, Eds., American Society for Testing and Materials, 1983, pp. 582-601.

5. Industrial Insulation 700 Series Plain and Faced, Owens/Corning Fiberglas Corp., Mechanical Division, Toledo, Ohio.

6. Darcy, H., "Les Fountaines Publiques de la Ville de Dijon," Dalmont, Paris, 1856.

7. Muskat, M, The Flow of Homogeneous Fluids through Porous Media, J. W. Edwadrs, Inc., 1946, p. 103.

8. Carman, P. C., "Fluid Flow through Granular Beds," Transactions of the Institution of Chemical Engineers, Vol. 15, 1937, pp. 150-166.

9. Wiggins, E. J., Campbell, W. B., and Maass, O., "Determination of the Specific Surface of Fibrous Materials," Canadian Journal of Research, Vol. 16, Sec. B., 1939.

10. Forchheimer, P. H., "Wasserbewegun durch Boden," Zeitschrift des Vereines Deutscher Ingenieure, Vol. 45, 1901, pp. 1782-1788.

11. Koh, J. C., Dutton, J. L., Benson, B.A., and Fortini, A., "Friction Factor for Isothermal and Non-isothermal Flow through Porous Media," Journal of Heat Transfer, Transaction of ASME, Vol. 99, August, 1977, pp. 367-373.

12. Beavers, G. S. and Sparrow, E. M., "Non-Darcy Flow through Fibrous Porous Media," Journal of Applied Mechanics, Transactions of the ASME, Vol. 47, December, 1969, pp. 711-714.

13. Ergun, S., "Fluid Flow through Packed Columns," Chemical Engineering Progress, Vol. 48, No. 2, February 1952, pp. 89-94.

14. Brownell, L. E., and Katz, D. L., "Flow of Fluids through Porous Media," Chemical Engineering Progress, Vol. 43, 1947, pp. 537-548.

15. Rose, H. E., "A Symposium of Papers on Flow of Fluids," Proceedings of the Institution of Mechanical Engineers, Vol. 153, No. 5, 1945, pp. 141-161.

16. Scheidegger, A. E., The Physics of Flow Through Porous Media, Third Edition, University of Toronto Press, 1974, pp. 133-136.

17. Ceaglske, N. H. and Hougen, O. A., "Drying Granular Solids," Industrial and Engineering Chemistry, Vol. 19, July, 1936, pp. 805-813.

18. Gray, W. G. and O'Neill, K., "On the General Equations for Flow in Porous Media and Their Reduction to Darcy's Law," Water Resources Research, Vol. 12, No. 2, April, 1976, pp. 148-155.

19. Whitaker, S., "Simultaneous Heat, Mass, and Momentum Transfer in Porous Media: A Theory of Drying," in Advances in Heat Transfer, Vol. 13, pp. 119-200, Academic Press, 1977.

20. Palosaari, S. M. and Cornish, A. R. H., "An Approximate Method for the Prediction of the Effective Thermal Conductivity of Wetted Porous Materials," Acta Polytechnica Scandinavica, Ch. 126, Helsinki, 1975, pp. 1-24.

21. Happel, J., "Viscous Flow Relative to Arrays of Cylinders," A.I.Ch.E. Journal, Vol. 5, No. 2, June 1959, pp. 174-177.

APPENDIX A

Recommended Test Procedure for Measuring the Hydraulic Conductivity of Fiberglass Insulations

These instructions are to be used in conjunction with the experimental apparatus described in Chapter II. The test procedure which follows is given to facilitate hydraulic conductivity measurements for insulation samples similar in structure to those studied in this investigation. The instructions are listed to permit quick and easy measurements and are provided in hopes that future experimenters in this area will experience none of the measurement problems that were encountered in this investigation.

Preliminary Preparation

1. Test samples should be cut slightly larger (approximately 3 mm) than the flow area. This ensures that no air becomes entrapped between the walls of the HC chamber and the insulation samples. Insulations which are less rigid require slightly larger test samples to secure a snug fit.
2. Wedge dry samples into the test section so that no air can become entrapped between successive insulation samples. Stack enough samples so that all pressure taps are measuring pressures within the upper and lower bounds of the stack. Attach manometers to the sides of the HC chamber.

3. While pouring water into the reservoir, turn on the recirculating pump and fill up the test section slowly with distilled water. Maintain a high level of water in the reservoir during fill-up operation. As the advancing water front gets near the lowest piece of insulation, adjust the throttle valve for minimum flow to allow the insulation to become fully and evenly saturated.
4. Once the advancing water front has cleared the top piece of insulation, position the overflow tubes to direct the flow back to the reservoir. Open up the throttle valve for maximum flow. This step helps drive air bubbles within the insulation to the free surface. Maintain this condition until all air is purged from the test samples.
5. With the recirculating pump shut off and the throttle valve closed, disconnect the tubing from the manometers and unscrew the pressure tap fittings. This liberates any further entrapped air from the test samples. Probe the pressure taps to make sure that no insulation fibers are blocking the flow of water into the manometer tubes. Reconnect the tubing. Refill the reservoir if the water level has lowered significantly.
6. Submerge the thermometer bulb into the water and secure it to the side of the HC chamber.
7. Adjust the manometer scales so that the level in each manometer tube indicates the same scale reading.

Experimental Procedure

8. Turn on the recirculating pump and adjust the throttle valve for minimum flow conditions. Record the rotameter reading, water temperature, and water levels in each of the manometer tubes.

9. Open up the throttle valve to cover a range of flow rates, recording the information in step 8 for each flow setting.

Reducing the Data

10. For any one flow setting, the hydraulic conductivity can be calculated using

$$K = \frac{\mu Q}{A} \quad \frac{h}{\rho g(h_2-h_1)} \tag{15}$$

where K = hydraulic conductivity, m^2

Q = volumetric flow rate, m^3/s

A = flow cross-sectional area, m^2

ρ = fluid density, kg/m^3

g = acceleration of gravity, 9.81 m/s^2

h_2-h_1 = difference in water levels between manometer tubes 1 and 2, mm

h = distance between pressure taps 1 and 2, mm

APPENDIX B

Cross-Check of HC Chamber Measurements

In order to cross-check hydraulic conductivity measurements, comparisons were made between results reported in the literature and those from the HC chamber. While a reference for measuring the hydraulic conductivity of a porous medium could not be found, a number of correlations is available in the literature for the pressure drop through granular solids, or more specifically, a packed bed of glass spheres. These correlations are based on experiments which employ a wide range of fluids and are conducted over laminar, transition, and turbulent flow regimes. While research in this area has yielded expressions which are quite different in form and predict widely different pressure drop values, two correlations applicable to the flow regime encountered in this investigation (Darcian) which are cited repeatedly are those of Carman (8) and Ergun (13).

Carman compiled the data of a number of contemporary researchers to yield the expression

$$\frac{\Delta p}{L} = \frac{\rho V^2 \psi S_t}{g\varepsilon^3} \tag{16}$$

where

$$\psi = 5 \left(\frac{\mu S}{\rho V} \right) + 0.4 \left(\frac{\mu S}{\rho V} \right)^{0.1} \tag{17}$$

Ergun proposed the correlation

$$\frac{\Delta p}{L} = 150 \frac{(1-\varepsilon)^2}{\varepsilon^3} \frac{\mu V}{D_p 2} + 1.75 \frac{(1-\varepsilon)}{\varepsilon 3} \frac{\rho V^2}{D_p} \qquad (18)$$

to quantify the pressure loss of a fluid which travels through a column packed with granular materials.

The HC chamber was packed with 6 mm diameter glass beads to form a volume approximately 200 mm x 200 mm x 100 mm. The pressure drop across the depth of this bed was measured by two pressure taps, spaced 50.8 mm apart, attached to inclined manometer tubes designed to improve the readability of the small pressure differential measurement. The data for a number of different flow rates are given in Table 6.

In order to compare the present results with the correlations by Carman and Ergun, it was necessary to measure the porosity of the packed beds. This parameter was determined using the formula

$$\varepsilon = \frac{\text{void volume}}{\text{bulk volume}} = \frac{\frac{1}{\rho 3}\left[\begin{array}{l}\text{mass of water needed to}\\ \text{completely submerge the}\\ \text{bed of glass spheres}\end{array}\right]}{\text{bulk volume of packed bed}} \qquad (19)$$

Because of the uncertainty involved in the measurement of both the bulk and void volumes, successive porosity measurements conducted in the laboratory differed by as much as 25 per cent for the same packed bed. These uncertainties resulted in porosity values in the range of $\varepsilon = 0.29$ to $\varepsilon = 0.37$ for the data in Table 6.

Table 6. Pressure Drop through a Packed Bed of 6 mm Diameter Glass Spheres

T (C)	V (m/s)	$\Delta p/L$ (Pa/m)
18	0.00153	216
18	0.00224	279
18.5	0.00261	417
18.5	0.00313	451
18.5	0.00354	480
19	0.00388	495
19	0.00422	559
19	0.00459	588

The Carman and Ergun correlations for the limiting cases of ϵ = 0.29 and ϵ = 0.37 are plotted in Fig. 17, along with the data points of Table 6.

As can be seen, the measurement of porosity plays an important role in quantifying the pressure drop through a packed bed of glass spheres. The porosity appears in both correlations raised to the third power. The data points in this exercise satisfactorily fall within the bounds prescribed by both the Ergun and Carman correlations. With the HC chamber properly cross-checked, it becomes possible to confidently measure the hydraulic conductivities of insulations studied in this investigation.

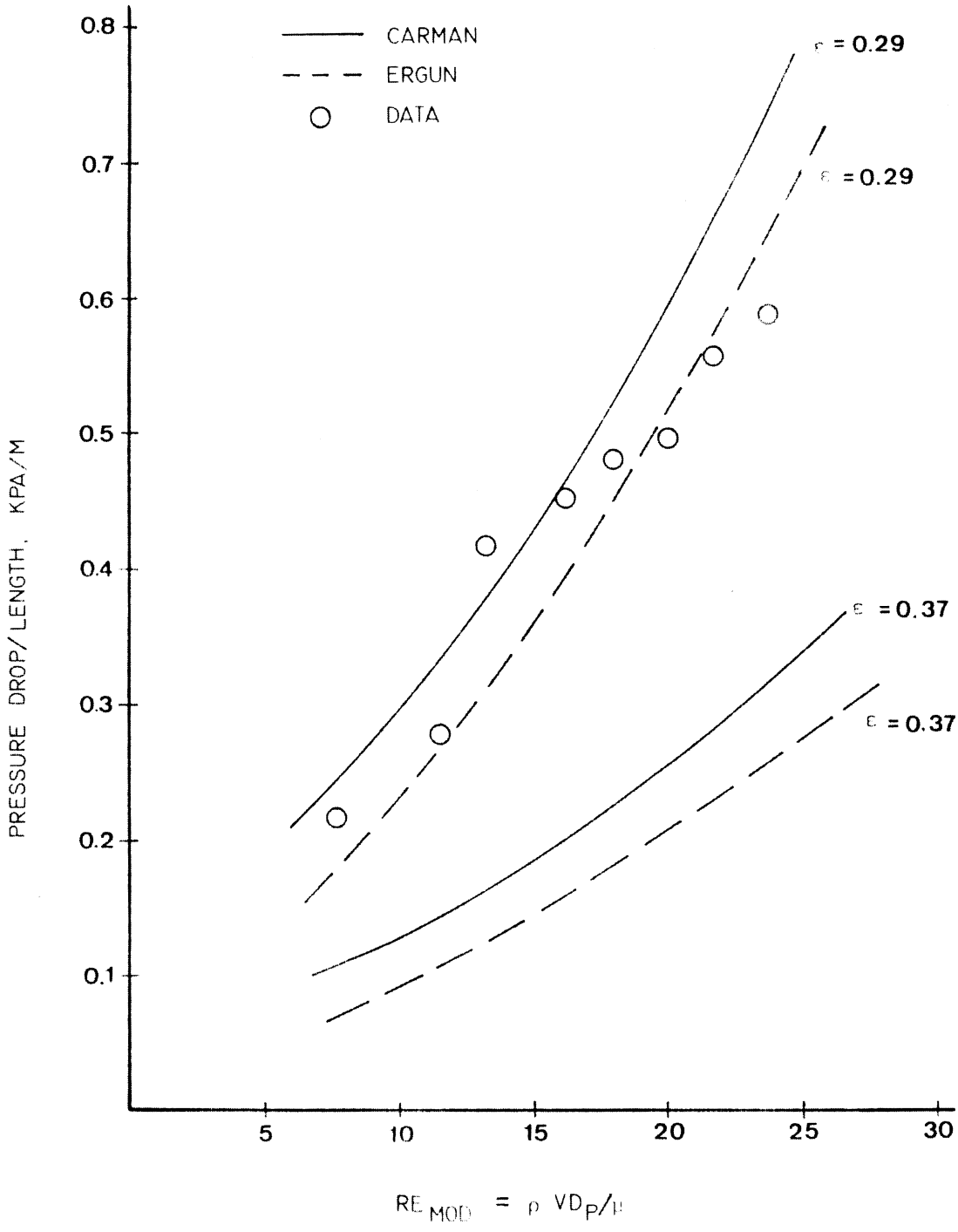

Figure 17. Pressure Drop through a Packed Bed of Glass Spheres.

APPENDIX C

Typical Pressure Drop Data

Typical Pressure Drop Data for Insulations A, B, and C are presented in the following tables.

Table C1. Pressure Drop through Insulation A. Sample 1.

Temp, T (C)	Density, ρ (kg/m^3)	Viscosity, μ (kg/m-s)	Mass Flow Rate, $\dot{m}$ (kg/s)	Pressure Drop, $\Delta p/L$ (kPa/m)
22	997.9	9.548×10^{-4}	0.0474	2.61
22	997.9	9.548×10^{-4}	0.0691	3.75
22.5	997.8	9.439×10^{-4}	0.1038	5.63
22.5	997.8	9.439×10^{-4}	0.1298	6.85
23	997.6	9.330×10^{-4}	0.1558	8.16
23	997.6	9.330×10^{-4}	0.1804	9.46
23	997.6	9.330×10^{-4}	0.2064	10.77
22.5	997.8	9.439×10^{-4}	0.0561	2.78
22.5	997.8	9.439×10^{-4}	0.0792	3.83
22.5	997.8	9.439×10^{-4}	0.1067	5.06
23	997.6	9.330×10^{-4}	0.1385	6.52
23	997.6	9.330×10^{-4}	0.1674	7.83
23	997.6	1.028×10^{-4}	0.1934	8.89

Table C2. Pressure Drop through Insulation A. Sample 3.

Temp, T (C)	Density, ρ (kg/m^3)	Viscosity, μ (kg/m-s)	Mass Flow Rate, $\dot{m}$ (kg/s)	Pressure Drop, $\Delta p/L$ (kPa/m)
25	997.2	8.908×10^{-4}	0.0517	2.61
25	997.2	8.908×10^{-4}	0.0835	4.07
25	997.2	8.908×10^{-4}	0.1153	5.54
25	997.2	8.908×10^{-4}	0.1413	6.69
25	997.2	8.908×10^{-4}	0.1659	7.83
25	997.2	8.908×10^{-4}	0.1962	9.21
23	997.6	9.330×10^{-4}	0.0546	2.94
24	997.4	9.111×10^{-4}	0.0864	4.49
24	997.4	9.111×10^{-4}	0.1168	6.03
24	997.4	9.111×10^{-4}	0.1428	7.34
24	997.4	9.111×10^{-4}	0.1717	8.65
24	997.4	9.111×10^{-4}	0.1991	10.03

Table C3. Pressure Drop through Insulation B. Sample 5.

Temp, T (C)	Density, ρ (kg/m^3)	Viscosity, μ (kg/m-s)	Mass Flow Rate, $\dot{m}$ (kg/s)	Pressure Drop, $\Delta p/L$ (kPa/m)
19.5	998.4	1.015×10^{-3}	0.0677	2.12
19.5	998.4	1.015×10^{-3}	0.0937	2.86
19.5	998.4	1.015×10^{-3}	0.1270	3.83
20	998.3	1.002×10^{-3}	0.1501	4.41
20	998.3	1.002×10^{-3}	0.1747	5.14
20	998.3	1.002×10^{-3}	0.1993	5.79
18.5	998.6	1.041×10^{-3}	0.0576	1.71
19.5	998.4	1.015×10^{-3}	0.0822	2.45
19.5	998.4	1.015×10^{-3}	0.1097	3.35
19.5	998.4	1.015×10^{-3}	0.1400	4.16
20	998.3	1.002×10^{-3}	0.1603	4.74
20	998.3	1.002×10^{-3}	0.1921	5.55

Table C4. Pressure Drop through Insulation B. Sample 6.

Temp, T (C)	Density, ρ (kg/m^3)	Viscosity, μ (kg/m-s)	Mass Flow Rate, $\dot{m}$ (kg/s)	Pressure Drop, $\Delta p/L$ (kPa/m)
22	997.9	9.548×10^{-4}	0.0633	1.71
22	997.9	9.548×10^{-4}	0.0850	2.29
22.5	997.8	9.439×10^{-4}	0.1139	3.18
22.5	997.8	9.439×10^{-4}	0.1385	3.67
22.5	997.8	9.439×10^{-4}	0.1602	4.32
23	997.6	9.330×10^{-4}	0.1789	4.73
23	997.6	9.330×10^{-4}	0.1992	5.38
23	997.6	9.330×10^{-4}	0.0590	1.80
23	997.6	9.330×10^{-4}	0.0792	2.29
23	997.6	9.330×10^{-4}	0.1067	3.02
23	997.6	9.330×10^{-4}	0.1341	3.67
23	997.6	9.330×10^{-4}	0.1587	4.32
23	997.6	9.330×10^{-4}	0.1761	4.81
23	997.6	9.330×10^{-4}	0.1948	5.22

Table C5. Pressure Drop through Insulation C. Sample 7.

Temp, T (C)	Density, ρ (kg/m^3)	Viscosity, μ (kg/m-s)	Mass Flow Rate, $\dot{m}$ (kg/s)	Pressure Drop, $\Delta p/L$ (kPa/m)
21	998.1	9.784×10^{-4}	0.0605	2.29
21	998.1	9.784×10^{-4}	0.0937	3.59
21	998.1	9.784×10^{-4}	0.1241	4.65
21	998.1	9.784×10^{-4}	0.1472	5.47
21	998.1	9.784×10^{-4}	0.1704	6.36
21	998.1	9.784×10^{-4}	0.2036	7.34
21	998.1	9.784×10^{-4}	0.0489	1.88
21	998.1	9.784×10^{-4}	0.0778	3.02
21	998.1	9.784×10^{-4}	0.1067	4.00
21	998.1	9.784×10^{-4}	0.1357	5.06
21.5	998.0	9.666×10^{-4}	0.1631	6.04
21.5	998.0	9.666×10^{-4}	0.1921	7.10

Table C6. Pressure Drop through Insulation C. Sample 9.

Temp, T (C)	Density, ρ (kg/m^3)	Viscosity, μ (kg/m-s)	Mass Flow Rate, $\dot{m}$ (kg/s)	Pressure Drop, $\Delta p/L$ (kPa/m)
17	998.9	1.081×10^{-3}	0.0576	2.45
17.5	998.8	1.067×10^{-3}	0.0822	3.59
17.5	998.8	1.067×10^{-3}	0.1126	4.90
18	998.7	1.053×10^{-3}	0.1444	6.21
18	998.7	1.053×10^{-3}	0.1705	7.35
18	998.7	1.053×10^{-3}	0.2023	9.06
18	998.7	1.053×10^{-3}	0.0475	2.04
18	998.7	1.053×10^{-3}	0.0721	3.10
18.5	998.6	1.041×10^{-3}	0.1010	4.25
18.5	998.6	1.041×10^{-3}	0.1270	5.39
19	998.5	1.028×10^{-3}	0.1560	6.53
19	998.5	1.028×10^{-3}	0.1834	7.68

APPENDIX D

A Simplified Model for Flow through an Assemblage of Cylinders

The photomicrographs of the samples studied in this investigation (Fig. 1) show that the fibers are randomly packed but generally lie in a plane perpendicular to the direction of flow. There is a considerable range of fiber diameters within any one sample. The random criss-crossing of fibers complicates any attempt to prepare a mathematical model to describe flow through the fiber matrix. An idealization of the fiber arrangement is in order. If the fiber matrix is envisioned as a network of uniform cylinders arranged in an ordered array, a mathematical description of the flow process becomes much easier. In an attempt to explain the fact that hydraulic conductivity values measured in this investigation did not increase for the less dense insulations, the following simplified model is proposed.

Happel (19) has proposed a free-surface model for viscous flow through assemblages of cylinders. His derivations are developed on the basis that two concentric cylinders can serve as the model for fluid moving through an assemblage of cylinders. The dimensions used by Happel in characterizing an arrangement of cylinders include

a = radius of cylindrical rod, transverse pitch

b = radius of cylindrical rod, cylindrical pitch

m = hydraulic radius (free volume/exposed area)

Happel relates these variables by the expression

$$m = \frac{b^2 - a^2}{2a} \tag{20}$$

By solving the Navier-Stokes equations for creeping flow in two dimensions, Happel arrives at an expression for the drag force on a single cylinder. In relating this drag force to the pressure gradient in the direction of flow and substituting into Darcy's Law, he obtains the following expression for the hydraulic conductivity:

$$K = \frac{b^2}{4}\left[\ell n \frac{b}{a} - \frac{1}{2}\left(\frac{b^4 - a^4}{b^4 + 4}\right)\right] \quad . \tag{21}$$

Consider a one cubic meter volume of insulation A ($\varepsilon = 0.9768$). A typical fiber diameter measures 12.0×10^{-6} m, as shown in Table 1. Assuming a fiber length of one meter, the volume occupied by one fiber is 1.23×10^{-10} m^3. In one cubic meter of insulation, the fibers take up $V_4''' = 1 - \varepsilon = 0.232$ m^3 of space. Therefore, the total number of fibers is about 1.89×10^8.

The hydraulic radius for a sample of insulation A is given by

$$m = \frac{\varepsilon \forall}{\pi d L N_f} \tag{22}$$

where L = fiber length (one meter)

N_f = total number of fibers

Substitution of the values presented above into Eq. 20 yields

$$m = \frac{0.9768\ (1m^3)}{\pi(12\times10^{-6}m)(1m)(1.89\times10^{8})} = 1.37 \times 10^{-4}\ m.$$

Substitution of $m = 1.37 \times 10^{-4}$ m into Eq. 20 yields $b = 4.10 \times 10^{-5}$m. The value of the hydraulic conductivity predicted by Happel is

$$K = \frac{(4.1\times10^{-5}m)^2}{4}\left[\ell n\ \frac{4.10\times10^{-5}m}{6.0\times10^{-6}m} - \frac{1}{2}\left[\frac{(4.10\times10^{-5}m)^4 - (6.0\times10^{-6}m)^4}{(4.10\times10^{-5}m)^4 + (6.0\times10^{-6}m)^4}\right]\right] = 5.98\times10^{-10}m^2$$

Calculations like the ones above were made for insulations B and C and are given in Table 7. As can be seen, measured values are of the same order of magnitude of those calculated using Eq. 21; however, the K-values given in Table 7 do not compare with the hydraulic conductivity trends measured in this investigation.

Further investigation is needed to correlate hydraulic conductivity measurements with other physical properties of fiberglass insulation. A detailed analysis of the variables affecting hydraulic conductivity determination is beyond the scope of the present investigation.

Table 7. Physical Characteristics of Flow through an Assemblage of Cylinders.

Insulation	Fiber Diameter, d (m)	ϵ	N_f	a (m)	b (m)	m (m)	K_{calc} (m^2)	K_{meas} (m^2)
A	12.0×10^{-6}	0.9768	1.89×10^{8}	6.0×10^{-6}	4.10×10^{-5}	1.37×10^{-4}	5.98×10^{-10}	5.04×10^{-10}
B	19.0×10^{-6}	0.9500	1.76×10^{8}	9.5×10^{-6}	4.25×10^{-5}	9.02×10^{-5}	4.51×10^{-10}	8.40×10^{-10}
C	20.5×10^{-6}	0.9450	1.67×10^{8}	10.3×10^{-6}	4.37×10^{-5}	8.80×10^{-5}	4.55×10^{-10}	6.55×10^{-10}

The vita has been removed
from the scanned document